Research Article

Israel Journal of Chemistry
www.ijc.wiley-vch.de

doi.org/10.1002/ijch.202300060

Another Torture Track for Quantum Chemistry: Reinvestigation of the Benzaldehyde Amidation by Nitrogen-Atom Transfer from Platinum(II) and Palladium(II) Metallonitrenes

Hendrik Verplancke,[a] Martin Diefenbach,[a, b] Jonas N. Lienert,[a] Mihkel Ugandi,[c] Marios-Petros Kitsaras,[d, e] Michael Roemelt,[c] Stella Stopkowicz,[d, e, f] and Max C. Holthausen*[a]

Dedicated to Prof. Helmut Schwarz on the occasion of his 80th birthday

Abstract: We showcase here a dramatic failure of CCSD(T) theory that originates from the pronounced multi-reference character of a key intermediate formed in the benzaldehyde amidation by N-atom transfer from Pd(II) and Pt(II) metallonitrenes studied recently in combined experimental and theoretical work. For detailed analysis we devised a minimal model system, for which we established reliable reference energies based on approximate full configuration interaction theory, to assess the performance of single-reference coupled-cluster theory up to the CCSDTQ(P) excitation level. While RHF-based CCSD(T) theory suffered dramatic errors, in one case exceeding 220 kcal mol^{-1}, we show that the use of broken-symmetry (BS) or Kohn-Sham (KS) orbital references yields substantially improved CCSD(T) results. Further, the EOM-SF-CCSD(T)(a)* approach met the reference data with excellent accuracy. We applied the KS-CCSD(T*)-F12b variant as high-level part of an ONIOM(KS-CC:DFT) scheme to reinvestigate the reactivity of the full Pt(II) and Pd(II) metallonitrenes. The revised reaction pathway energetics provide a detailed mechanistic rationale for the experimental observations.

Keywords: Computational Chemistry · Coupled-Cluster Theory · Electronic Structure · Nitrogen Atom Transfer · Singlet Biradicaloids

1. Introduction

Organic Nitrenes (R–N) are typically highly reactive monovalent nitrogen species involved as singlet or triplet intermediates in numerous important chemical transformations such as C–H amination or aziridination reactions.[1] The use of organic azides as convenient precursors enables catalytic transformations based on the corresponding transition metal complexes [M]–NR and recent studies provide comprehensive insight into electronic structure and mechanistic detail.[2] Transition metal nitrido complexes [M]≡N represent an interesting alternative source for nitrogen atom transfer reactions in principle. They have attracted substantial recent interest in the context of N_2 fixation,[3] but concepts to use these species to generate nitrogenous products are far less developed. Nitrido complexes with pronounced nitrenoid character have long been suggested as (fleeting) reactive intermediates in nitrogen atom transfer reactions.[4] However, examples for authentic

[a] *H. Verplancke, M. Diefenbach, J. N. Lienert, M. C. Holthausen*
Institut für Anorganische und Analytische Chemie, Goethe-Universität,
Max-von-Laue-Str.7, 60438 Frankfurt am Main, Germany;
E-mail: max.holthausen@chemie.uni-frankfurt.de
[b] *M. Diefenbach*
Fachbereich Chemie, Theoretische Chemie, Technische Universität Darmstadt,
Alarich-Weiss-Straße 4, 64287 Darmstadt, Germany
[c] *M. Ugandi, M. Roemelt*
Institut für Chemie, Humboldt-Universität zu Berlin,
Brook-Taylor-Straße 2, 12489 Berlin, Germany
[d] *M.-P. Kitsaras, S. Stopkowicz*
Department Chemie, Johannes Gutenberg-Universität Mainz,
Duesbergweg 10–14, 55128 Mainz, Germany
[e] *M.-P. Kitsaras, S. Stopkowicz*
Fachrichtung Chemie, Universität des Saarlandes,
Campus B2.2, 66123 Saarbrücken, Germany
[f] *S. Stopkowicz*
Hylleraas Centre for Quantum Molecular Sciences, Department of Chemistry, University of Oslo, P.O. Box 1033, N-0315 Oslo, Norway

Supporting information for this article is available on the WWW under https://doi.org/10.1002/ijch.202300060

terminal metallonitrenes [M]–N, metal analogs of organic nitrenes featuring monovalent atomic nitrogen ligands, have been established only recently by photocrystallographic, magnetic and quantum-chemical characterization.[5] After photolysis of an azide precursor, a transient ground-state triplet Pt^{II}–N species was shown to swiftly undergo various N-atom transfer reactions. Detailed experimental and computational studies of the stoichiometric aldehyde amidation revealed a nucleophilic attack of the metallonitrene at the carbonyl group with an inverted selectivity compared to the common electrophilic nitrene transfer observed for organic homologs N–R.[5a] In most recent work, a photocatalytic protocol for silylamidation of aldehydes was devised based on the corresponding Pd(II) pincer platform, which provides convenient access to primary amides.[5b] We found substantial similarities between the Pt and the Pd complexes with respect to molecular and electronic structure but encountered unexpectedly severe problems during quantum-chemical reactivity studies of the latter, which lead us to conclude that also the results for the Pt system could not be trusted. We will expand on these problems, identify their origins, and suggest pragmatic solutions in the present contribution.

The coupled-cluster (CC) singles and doubles with perturbative triples model, CCSD(T),[6] is widely regarded as the gold standard of (black-box) quantum chemistry.[7] Commonly based on a single Hartree-Fock (HF) determinant as reference wave function, this method often provides excellent accuracy for molecular thermochemistry and kinetics if combined with large, highly polarized basis sets used within a suitable complete basis set (CBS) limit extrapolation procedure. Yet the computational effort for such calculations becomes prohibitive even for moderately sized molecules comprising, say, 10–15 heavy atoms, owing to its formal seventh-order scaling with the system size (*viz.* the number of correlated electrons). Modern developments based on fragment procedures,[8] localized molecular orbitals,[9] or machine learning,[10] thus aim at breaking the scaling wall while maintaining exquisite accuracy. Common wisdom has it, however, that all these methods hold promise only if the system under study is sufficiently well described by the reference wave function used and if static correlation effects remain moderate. To some extent such problems can be detected by interpretation of coupled-cluster diagnostics such as the size of t_1 amplitudes, commonly condensed into the $\mathcal{T}_1$ diagnostic (a measure for the quality of the reference orbitals), or the size of t_2 amplitudes (a measure for multi-reference character).[11]

For some years we have been applying the CCSD(T) method very successfully as part of a two-layer ONIOM approach to investigate the thermochemistry and kinetics of moderately large transition metal complexes, for which DFT failed to provide sufficient accuracy.[3g,12] The ONIOM approach separates a smaller model system, containing the electronically demanding regions, from the real system that is too large for a treatment at a sufficiently high level of theory. A mechanical embedding scheme then allows to extrapolate the high-level description of the model system to the entire molecule.[13] Specifically, to ameliorate the extensive growth of computational effort with the basis set size we routinely employed the explicitly correlated CCSD(T*)-F12b ansatz as high-level method, which has been designed to provide results of CBS-limit quality in combination with moderately sized basis sets.[14]

In our quantum-chemical assessment of the Pt(II) nitrene reactivity with benzaldehyde (Scheme 1) we have used the ONIOM(CC-F12:DFT) approach to compensate for known DFT shortcomings identified in related studies.[5a,15] Although we observed borderline $\mathcal{T}_1$ diagnostics for some stationary points along the reaction pathways studied, the results seemed nevertheless acceptable based on a favorable comparison with multi-reference NEVPT2 theory.[5a] For the closely related palladium analog, however, the CCSD(T*)-F12 part of the

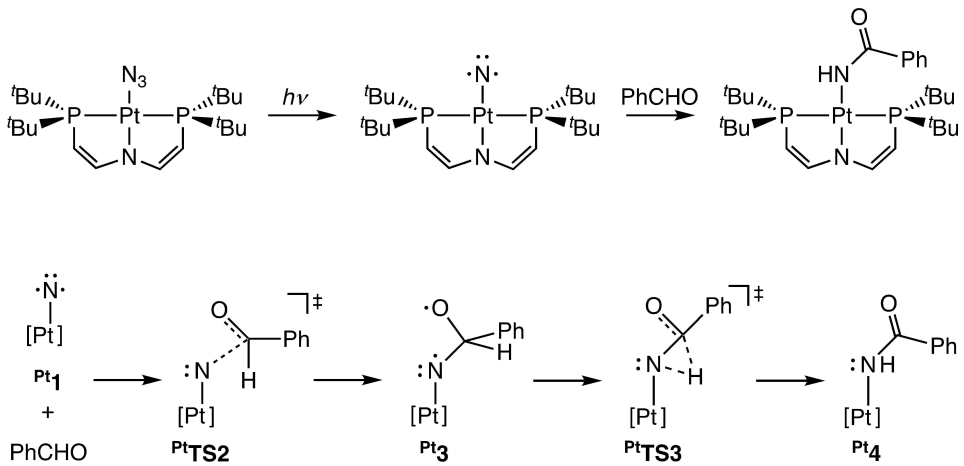

Scheme 1. Stoichiometric benzaldehyde amidation by N-atom transfer from Pt(II) metallonitrene ^{Pt}**1** (top) and sketch of computed key elementary steps (bottom).[5a]

ONIOM approach led to a dramatic overstabilization of a key intermediate (^{Pd}**3**, see below), with alarmingly large (T*) contributions exceeding 70 kcal mol^{-1} in relative energy. Obviously, the biradicaloid singlet character of these species represents a challenging tipping point for the applicability of single-reference coupled-cluster theory. While some case studies on species with moderate biradical character suggest that CCSD(T) theory can compensate for deficits of the HF single-determinant wave functions to some extent,[16] a robust assessment of systems with stronger near-degeneracy effects typically requires much higher CC excitation levels or application of genuine multi-reference approaches.[17] With the latter methods, however, a balanced description of dynamic and non-dynamic correlation effects required for reactivity studies is a non-trivial and computationally taxing enterprise even for small molecules. As an alternative, equation-of-motion coupled-cluster (EOM-CC) theory,[18] and – particularly well-suited for the assessment of biradicals – its spin-flip variant (EOM-SF-CC)[19] represents a conceptually robust single-reference approach to properly describe multi-configurational problems. In this context, the EOM-SF-CCSD(T)(a)* variant, which combines non-iterative triples[20] with the EOM-SF scheme, holds particular promise to bring 'gold-standard' accuracy within reach.

In the DFT realm, in turn, a substantial body of work bears witness that biradical systems can successfully be addressed with great computational efficiency by means of the broken-symmetry (BS) approach.[21] Motivated by a few reports on the successful application of BS-CC theory to related problems,[22] we adopted this route here. As an interesting alternative we also tested the use of Kohn-Sham (KS) reference orbitals for coupled-cluster theory. This approach has received considerable attention in past decades and numerous reports have been put forth on beneficial effects of using DFT orbitals as reference for perturbation theory, configuration interaction, and coupled-cluster computations.[23]

In the following we show by comparison to approximate full configuration interaction (FCI) data obtained for a minimal model system that the use of BS or KS orbital references for limited CC expansions as well as EOM-SF-CC can yield substantially improved results in cases where conventional RHF-based CC theory fails miserably, even exceeding the error margins observed for critically acclaimed torture track cases of the past.[16e,24] As the KS-CCSD(T) approach is technically easy to realize in many available quantum chemistry programs we recommend it as a robust method to master intricate electronic structure problems with moderate multi-reference character. We show that in particular perturbative triples contributions, which have provided dramatically flawed results for biradicaloid singlet species using conventional HF orbitals, profit substantially from the use of a KS orbital reference. This is a notable finding in view of the critical importance of (T) contributions to reach chemical accuracy by means of CCSD(T) theory.[6,25] We show below how the results obtained for a small molecular model can be extrapolated to the real metal complexes by a two-layer ONIOM procedure and we establish in this way reaction pathway energetics for the Pd(II) and Pt(II) nitrene reaction with benzaldehyde, the latter results replacing earlier work.

2. Quantum Chemical Methods

Geometry optimizations and analytic Hessian evaluations were performed with the Gaussian 16 program.[26] Here, the PBE0 hybrid functional[27] was employed together with the D3 empirical dispersion correction with Becke-Johnson damping.[28] For the metal complexes, the def2-SVP basis set[29] was used including a quasi-relativistic pseudopotential for the Pd and Pt atoms.[30] Calculations on the minimal model system ($HN+CH_2O$) were performed with the def2-TZVPP basis set[29] and with the superfine integration grid. Contributions to Gibbs free energies were evaluated at stationary points employing the standard routines of Gaussian 16 and used as incremental correction to single point energies obtained at more sophisticated levels of theory. Calculations on singlet states for **TS2**, **3**, **TS3**, and **TS4** (see below) were performed employing spin-unrestricted, broken-symmetry wave functions for geometry optimizations and projected singlet energies (E_S) were obtained from calculated triplet (E_T) and broken-symmetry singlet (E_{BS}) energies and the corresponding $\langle S^2 \rangle$ expectation values according to Yamaguchi, Equation 1:[17d,21p]

$$E_S = E_T - \frac{2(E_T - E_{BS})}{\langle S^2 \rangle_T - \langle S^2 \rangle_{BS}} \quad (1)$$

Energy decomposition analysis with natural orbital for chemical valence (EDA-NOCV, also known as ETS-NOCV)[31] was performed with the ADF 2019[32] program employing the PBE0 functional in combination with the triple-ζ Slater-type basis set TZ2P.[33]

Coupled-cluster calculations were performed with the programs Gaussian 16,[26] ORCA 4.2.1,[34] Molpro 2015,[35] CFOUR 2.1,[36] Qcumbre,[37] GAMESS 2021 R2,[38] MRCC 2020[39] and MRCC 2022 (the latter 2022 version for KS-CC calculations performed with MRCC, which included an important improvement for the use of alternative orbital references). The frozen core approximation was employed throughout and only valence electrons were included in the correlation treatment. The explicitly correlated CCSD(T*)-F12b variant[14] with the cc-pVTZ-F12 basis set[40] (aug-cc-pVTZ-PP for Pd and Pt)[41] was used as implemented in Molpro, in which the (T*) perturbative triples contributions are improved towards the complete basis set limit via F12-scaling[42] using the scale factor E_{corr}(MP2-F12)/E_{corr}(MP2). The corresponding JKfit triple-zeta auxiliary basis sets,[43] the MP2fit sets for density fitting, and the OptRI/JKfit sets for construction of the complementary auxiliary basis sets (OptRI for non-metal atoms, JKfit for Pd and Pt) were used. Technically, CCSD(T) calculations with DFT or CASSCF orbitals were performed with the Molpro program by feeding PBE0,[27] BP86,[44] or full valence CASSCF wave functions

into the Hartree-Fock routine, with the number of iterations set to zero, followed by the coupled-cluster calculation. This approach yields a non-self-consistent HF-type reference energy and the original DFT or CASSCF orbital energies are passed to the coupled-cluster module. PBE0-CCSD up to PBE0-CCSDTQ(P) calculations with the ano-pVDZ basis set were performed with the MRCC 2022 code.

CCSDT,[45] CCSDT(Q),[46] CCSDTQ,[47] and CCSDTQ(P)[46b,c] calculations employing the ano-pVDZ,[48] cc-pVDZ,[49] cc-pVTZ,[49] and cc-pVQZ[49] basis sets were performed with the MRCC program package. The CFOUR program was used for coupled-cluster calculations with broken-symmetry UHF reference determinants and coupled-cluster $\langle S^2 \rangle$ expectation values were used for spin-projection according to Equation 1. Specifically, for CCSD(T) rigorous coupled-cluster $\langle S^2 \rangle$ expectation values[50] were used, which require analytic gradient evaluation, whereas at the CCSDT level only projected $\langle S^2 \rangle$ expectation values are available. For ^{H}**3a** and ^{H}**3b** comparison of both variants computed at the CCSD level gave only minor deviations below 0.05, with insignificant impact (< 0.2 kcal mol^{-1}) on singlet energies obtained by Yamaguchi's spin-projection procedure. For the critical case of singlet imidogen substantial deviations between those measures were observed, connected to convergence of BS-CC to the triplet state (see below). CBS extrapolation of spin-projected total energies was performed by solving the system of linear equations for cardinal numbers 2, 3, and 4 following Peterson *et al.* (Equation 2).[51]

$$E_X = E_{\mathrm{CBS}} + \mathrm{A}e^{-(X-1)} + \mathrm{B}e^{-(X-1)^2} \tag{2}$$

BS-CC calculations on the palladium and platinum systems were performed with the ORCA program, employing the def2-SVP, def2-TZVPP and def2-QZVPP basis sets[29] including quasi-relativistic pseudopotentials for Pd and Pt.[30] As $\langle S^2 \rangle$ expectation values for the coupled-cluster wave function are unavailable within the ORCA program, spin-projection was performed according to Noodleman,[21b] Equation 3, representing the weak coupling limit of spin-spin interactions (i.e. expected $\langle S^2 \rangle$ values near 1.0 for the BS singlet solution), and the resulting total energies were used for CBS extrapolation according to Equation 2.

$$E_{\mathrm{S}} = E_{\mathrm{T}} - 2(E_{\mathrm{T}} - E_{\mathrm{BS}}) \tag{3}$$

The CCSD(T) test calculations for a minimal model system (see below) have shown that Molpro, CFOUR, ORCA, Gaussian, GAMESS, Qcumbre and MRCC converge to the same solution, except for structure ^{H}**3a** (*vide infra*). 3ζ and 4ζ correlation energies were extrapolated to the CBS limit according to Equation 4.[48]

$$E_{\mathrm{CBS}} = \frac{4^{3.05}E_{4\zeta}^{\mathrm{corr}} - 3^{3.05}E_{3\zeta}^{\mathrm{corr}}}{4^{3.05} - 3^{3.05}} + E_{4\zeta}^{\mathrm{HF}} \tag{4}$$

BD(T)[52] calculations (Brueckner doubles with perturbative triples corrections) with the ano-pVDZ basis set were performed with the Gaussian 16 program. Orbital-optimized OO-MP2 calculations with the ORCA program were performed employing the ano-pVDZ basis set and the resolution of identity (RI) approximation with the automatically generated auxiliary basis sets (autoaux keyword).[53] These orbitals were fed through the HF routines without further optimization (NoIter keyword) and used as reference for CCSD(T) computations. This approach yields a non-self-consistent HF-type reference energy and the OO-MP2 orbitals are passed to the coupled-cluster module. The completely renormalized coupled-cluster variant CR-CC(2,3) devised by Piecuch and coworkers, also referred to as CR-CCSD(T)L,[54] was employed as implemented in GAMESS in combination with the ano-pVDZ basis set. Equation of motion CCSD for electronic excitation (EOM-EE-CCSD) calculations with the ano-pVDZ basis set were performed with the CFOUR or the ORCA implementations, depending on the chosen reference determinant. Excitation energy (EE) and spin-flip (SF)[19a,c,55] EOM-CC calculations employing the EOM-EE-CCSD, EOM-SF-CCSD and EOM-SF-CCSD(T)(a)*[20] methods with the ano-pVDZ, cc-pVDZ, cc-pVTZ and cc-pVQZ basis sets were performed with the Qcumbre program.[37] CBS extrapolation of total energies was performed according to Equation 2.

For improved single point energy calculations on the full molecular platinum and palladium complexes we employed a subtractive two-layer ONIOM extrapolation approach,[13] constructing the model system based on the DFT-optimized full molecular system by replacing the pincer ^{t}Bu groups and the phenyl group of the benzaldehyde substrate by hydrogen atoms aligned along the P–C and C–C bonds broken (Figure 1). The resulting P–H and C–H bond lengths were relaxed at the DFT level while keeping all other model system coordinates fixed. Single point energy calculations were then performed on the model system at the KS-CCSD(T*)-F12/VTZ-F12 level ('high level', HL) and at the PBE0-D/def2-TZVPP level ('low level', LL), which was also used to obtain single point energies for the full ('real') system.[56] Combina-

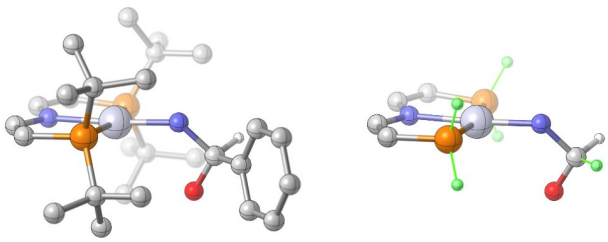

Figure 1. Illustration of molecular structures used in ONIOM extrapolations (left: real system ^{Pt}**3**, right: H-truncated model system (^{Pt}**3**)^{model}); most hydrogen atoms omitted for clarity, additional H atoms introduced into the model system to saturate broken covalent bonds highlighted in green.

tion of the three energies according to Equation 5 introduces a 'high level' description of the model system, which comprises the challenging electronic structure problem, while the remaining parts of the real system are represented at the 'low level'. To a good approximation the subtractive scheme cancels effects of the additional H atoms introduced to saturate covalent bonds broken upon construction of the model system.

$$E_{\mathrm{ONIOM(HL:LL)}} = E_{\mathrm{LL}}^{\mathrm{real}} - E_{\mathrm{LL}}^{\mathrm{model}} + E_{\mathrm{HL}}^{\mathrm{model}} \quad (5)$$

The strongly contracted NEVPT2[57] variant was used as implemented in ORCA 4.2.1 based on state-specific full valence CASSCF wave functions together with the ano-pVDZ basis set. Approximate full configuration interaction (FCI) energies for CH_2O and the distinct electronic states of ^{H}**3** were computed employing the FCI Quantum Monte Carlo (FCIQMC) method[58] including the semi-stochastic,[59] initiator[60] and adaptive-shift[61] extensions as implemented in the program package NECI.[62,63] To ensure convergence to the wave function of interest, the spin purification approach was employed for computation of the ^{1}A" states.[64] The starting FCIDUMP files were generated with the ano-pVDZ basis set using the Molpro program package. Only valence electrons were included in the correlation treatment. For imidogen (NH) the canonical FCI energy with the ano-pVDZ, cc-pVTZ and cc-pVQZ basis sets was computed with Molpro accordingly. To ensure convergence to the FCI energy, FCIQMC computations were iteratively repeated with an increasing number of walkers (10^7–$2\cdot10^9$).[65] The correlation energies and stochastic error bars were obtained by manual blocking analysis including the iterations after the completion of the walker growth and equilibration phases. An overview of all FCIQMC runs and blocking analyses is provided as supporting information.

Accompanying the FCIQMC calculations, approximate FCI energies were computed with a recently developed selected CI approach,[66] which makes use of the heatbath CI (HCI) selection algorithm of Umrigar and coworkers.[67] The HCI method used in this work is implemented in the MOLBLOCK program[68] and relies on a configurational basis, where spin-adaptation is taken care of by an implicit configurational state function basis during the construction of electronic coupling coefficients.[69] The spin pure nature of the method avoids possible errors arising from spin contamination or even convergence to a wrong spin state as might occur with methods that employ a Slater-determinant basis. The final HCI energies were obtained with tight thresholds: $T_{gen} = 4\cdot10^{-3}$, $T_{var} = 1\cdot10^{-6}$, $T_{PT2} = 1\cdot10^{-7}$. As outlined elsewhere, these thresholds control the size of the variational and perturber space, respectively.[66] The corresponding starting orbitals were taken as the natural orbitals from a HCI calculation with less tight thresholds: $T_{gen} = 1\cdot10^{-2}$, $T_{var} = 1\cdot10^{-5}$, $T_{PT2} = 1\cdot10^{-6}$.

3. Results

As detailed in the introduction we have encountered unexpectedly severe problems with the ONIOM(CC:DFT) description of intermediate ^{Pd}**3**, which is formed by initial attack of the nitrene at the aldehyde carbon atom. In the following section we provide a detailed analysis of the underlying electronic structure problem for a minimal model system comprising imidogen and formaldehyde. This minimal model captures the essence of the electronic structure problem of the full transition metal complexes. Both the model and the real systems exhibit substantial singlet wave-function instabilities caused by orbital near degeneracies; the resulting biradical(oid) character of the intermediate is localized completely on the organic N–C–O fragment also for the metal complexes. Further details, such as Cartesian coordinates of molecular structures, total energies, and analysis of wave-function contributions, are provided as Supporting Information.

3.1 Electronic Structure of the Minimal Model System

The $1\sigma^2 2\sigma^2 3\sigma^2 1\pi^2$ electron configuration of imidogen NH gives rise to a $^3\Sigma^-$ ground state and a lowest excited state of $^1\Delta$ character, energetically well separated by an adiabatic singlet-triplet splitting $\Delta E_{S-T} = 36.3$ kcal mol^{-1} as determined in stimulated emission pumping experiments.[70] The model reaction studied here starts by initial side-on attack of triplet imidogen to formaldehyde and bond formation involves interaction of a singly occupied π orbital of the former with the π bond of the latter. More precisely, a detailed EDA-NOCV bonding analysis of the associated transition state ^{H}**TS2** shows that pairing of an α electron in the in-plane imidogen π-orbital with a β electron in the bonding C=O π-orbital leads to formation of the N–C σ bond, leaving an unpaired α electron at O (Figure 2).

The resulting intermediate ^{H}**3** thus represents a diradical with spin-densities essentially localized at the N and O atoms giving rise to energetically close lying singlet and triplet states. Moreover, as detailed in Figure 3 we identified two electromers for each spin state, ^{H}**3a** and ^{H}**3b**, resulting from different occupation patterns of the frontier molecular orbitals: the π_1 and π_2 orbitals both comprise the out-of-plane p AOs at N and O and the corresponding in-plane p orbital at oxygen is part of a σ antibonding interaction. The minute energy difference between the doubly occupied σ and π_1 orbitals, together with the low-lying π_2 LUMO, indicates a near degeneracy situation, resulting in a biradicaloid singlet instability of the RKS wave function.

Correspondingly, in ^{H}**3a** the σ orbital and the π_2 are singly occupied and we find a ^{3}A" ground state for this species separated by 6.1 kcal mol^{-1} from its biradicaloid ^{1}A" state. The biradicaloid ^{1}A' ground state of ^{H}**3b**, in turn, results from single occupation of the two π_1 and π_2 MOs, with the related triplet residing merely 3.7 kcal mol^{-1} above. Near the mini-

Israel Journal of Chemistry

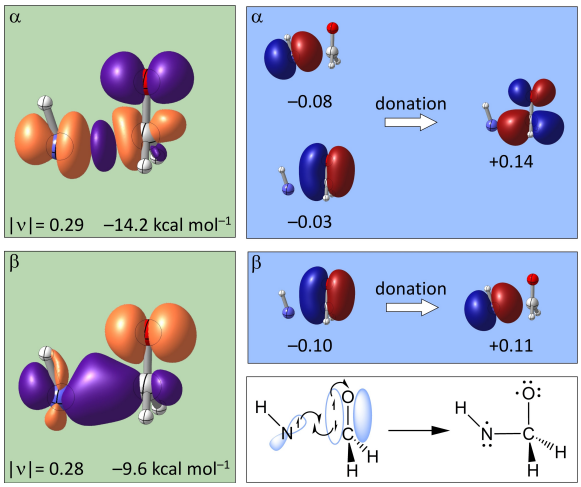

Figure 2. EDA-NOCV deformation densities of triplet ^{H}**TS2** (green panels), corresponding donor and acceptor symmetrized fragment orbitals (SFOs, blue panels) with mixing coefficients, and a more intuitive Lewis representation of interacting fragments. Deformation densities shown at $\pm 0.002\ a_0^{-3}$ (density depletion in orange and accumulation in purple), SFO isosurfaces at $\pm 0.05\ a_0^{-3/2}$.

mum geometry of ^{H}**3a**, however, the ^{1}A' state is nearly degenerate with the ^{1}A" potential energy surface (cf. Figure 3). Obviously a physically correct representation of both singlet states requires a two-determinantal treatment at least, as does the representation of the $^{1}\Delta$ state of NH with its strictly degenerate π-orbitals, which is part of the singlet fragmentation asymptote.[15c,71] In this context we note that these model system singlet species feature all relevant aspects of the electronic intricacies of the full molecular system.

Whenever a single determinant fails to provide a suitable reference description for such situations, fundamental problems can arise for standard coupled-cluster methods like CCSD(T). While the use of ever higher excitation patterns will eventually establish invariance with respect to the quality of the reference wave function, also in critical cases, further scrutiny is needed to establish the validity of a CCSD(T) description based on a single RHF reference. In the following we evaluate two unconventional approaches to resolve these problems, that is, the use of a KS orbital reference and broken-symmetry coupled-cluster theory.

It has been shown that the use of unrestricted wave functions with broken space and spin symmetry can recover critical near-degeneracy correlation effects,[17d,21p] and in view of the fact that broken-symmetry UHF solutions have a well-established physical basis[72] we note a curious lack of relevant literature as to the use of even electron[73] broken-symmetry reference wave functions for coupled-cluster methods. To the best of our knowledge only the groups of Yamaguchi, Bartlett, and Stanton reported detailed work along these lines.[22] We put this option to the test further below.

Based on DFT-optimized structures we use energies obtained by Alavi's approximate full configuration interaction quantum Monte Carlo method (FCIQMC)[58–61,64] with the ano-pVDZ basis set as a benchmark (Table 1). Due to this only moderately sized basis set the singlet/triplet gap computed for imidogen deviates by 5.0 kcal mol^{-1} from the experimentally determined adiabatic value (36.3 kcal mol^{-1}). With respect to separated imidogen and formaldehyde the ^{3}A" ground state of ^{H}**3a** is less stable by 2.7 kcal mol^{-1}, while the ^{1}A' ground state of ^{H}**3b** lies 2.1 kcal mol^{-1} below the fragment asymptote. Our results obtained with the deterministic HCI method agree quantitatively with these findings (Table 1). The fact that the two fundamentally different approximations to FCI agree within a narrow margin lends weight to our choice of FCIQMC as benchmark method. Yet at this point we emphasize again the importance of using the spin-purification routines newly implemented in the NECI program[64] – initial Slater-determinant based FCIQMC calculations on the ^{1}A"

Table 1. Computed relative energies for the singlet and triplet states of ^{H}**3a** and ^{H}**3b** referenced to separate triplet imidogen (^{H}**1**) and formaldehyde and singlet-triplet energy difference for ^{H}**1** in kcal mol^{-1}; FCIQMC/ano-pVDZ reference data (boldface) and deviations $\Delta\Delta E_{rel}$ obtained with the spin-adapted HCI method and several coupled-cluster variants with the ano-pVDZ basis set are given as well. Data based on PBE0/def2-TZVPP optimized structures.

Method	^{H}**1** ΔE_{S-T}	^{H}**3a** ^{1}A"	^{1}A'[c]	^{3}A"	^{H}**3b** ^{1}A'	^{3}A'
FCIQMC	**41.3**	**8.8**	**7.9**	**2.7**	**−2.1**	**1.6**
HCI	0.0	−0.7	−0.2	0.2	0.0	0.1
CCSD[a]	8.7	–[b]	70.9[d]	0.6	21.7	−0.4
CCSD(T)[a]	5.4	–	68.8[d]	0.9	−9.6	0.5
CR-CC(2,3)[a]	4.8	–	69.1[d]	0.3	5.6	0.2
CCSDT[a]	0.3	–	69.2[d]	−0.1	2.6	−0.2
CCSDT(Q)[a]	−0.1	–	67.1[d]	−0.1	−3.6	0.0
CCSDTQ[a]	0.0	–	69.1[d]	−0.1	0.1	−0.1
CCSDTQ(P)[a]	0.0	–	69.6[d]	−0.1	−0.2	0.0

[a] CR-CC(2,3) calculations performed with GAMESS and all other coupled-cluster calculations with MRCC; [b] ^{1}A" state symmetry not accessible with an RHF reference; [c] At the structure of ^{H}**3a**, the excited ^{1}A" state is nearly degenerate with the biradicaloid ^{1}A' state, which is the ground state of ^{H}**3b** (cf. Figure 3); [d] convergence to a high-lying ^{1}A' excited state.

Israel Journal of Chemistry

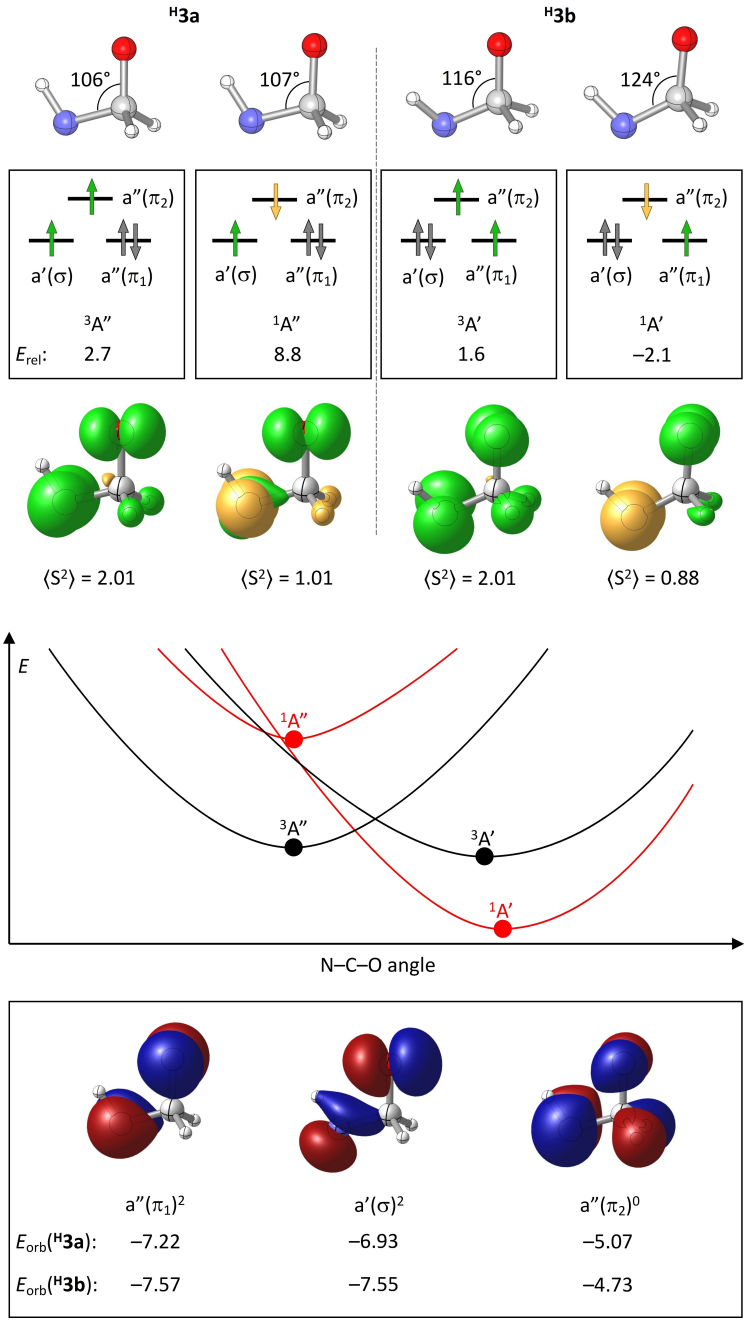

Figure 3. Molecular structures, schematic orbital occupation and spin-density plots for the two triplet and the two singlet electromers ^{H}**3a** and ^{H}**3b** (top), rough sketch of the pertinent potential energy surface sections (center) and PBE0 molecular orbitals from an RKS calculation on singlet ^{H}**3a** (bottom). FCIQMC energies are given in kcal mol^{-1} relative to separated imidogen and formaldehyde. Spin-density isosurfaces at ± 0.01 a_0^{-3}, MO isosurfaces at ± 0.05 $a_0^{-3/2}$ and orbital energies in eV (orbital energies for ^{H}**3b** are given for comparison, the respective orbitals closely resemble those shown for ^{H}**3a**). Further details of molecular structures are provided in the Supporting Information.

state of ^{H}**3a** converged to its corresponding triplet ground state.

Turning to the coupled-cluster data, we note significant deviations for CCSD and CCSD(T) results for the singlet/triplet gap of imidogen and only inclusion of higher-level electron correlation effects from iterative triple excitations on leads to convergence to the FCI limit. While the triplet states of ^{H}**3a** and ^{H}**3b** do not challenge coupled-cluster theory at any level, the singlet states with their inherent multi-reference character do: for ^{H}**3b** substantial errors, oscillating about the FCI value, are observed up to CCSDT(Q) and only higher excitation levels show convergence to the FCI limit. The large

deviations of no less than 67 kcal mol^{-1} for ^{H}**3a** go back to the fact that the CCSD wave function obtained with MRCC corresponds to a high lying ^{1}A' excited state. In fact, using various quantum chemistry program packages one of two distinct solutions were obtained, depending on the program. Employing default program control settings throughout, calculations with MRCC, CFOUR, Qcumbre and GAMESS, all converged to the same high-lying ^{1}A' state, while a drastically different solution was consistently obtained with Molpro, Gaussian and ORCA (Table 2). Employing the latter programs, the CCSD wave function converges instead to a biradicaloid ^{1}A' state, much lower in energy.[74] As expected for the multi-reference problem at hand,[11] this biradicaloid solution features a critically large leading t_2 amplitude of 0.91, exceeding the limit of 0.20 usually seen as well-behaved,[75] a similarly large leading t_1 amplitude of 1.02 (leading amplitudes indicate associated $\pi_1 \rightarrow \pi_2$ excitations), and an excessively large $\mathcal{T}_1$ diagnostic of 0.24, hugely exceeding the recommended limit of 0.02.[76]

However, a small negative excitation energy of −2.8 kcal mol^{-1} obtained in an EOM-EE-CCSD calculation with this reference identifies yet a lower lying ^{1}A" biradicaloid state (see Supporting Information), at variance with the FCIQMC state ordering. The biradicaloid ^{1}A' solution for ^{H}**3a** exhibits unphysically large perturbative triples contributions of more than 250 kcal mol^{-1}, denoting the breakdown of CCSD(T) here. For the high-lying excited ^{1}A' CCSD solution obtained with CFOUR (or MRCC, Qcumbre, and GAMESS) we find a large, though less alarming leading t_1 amplitude of 0.39 ($\pi_1 \rightarrow \pi_2$ single excitation), a $\mathcal{T}_1$ diagnostic of 0.10, but innocuous t_2 amplitudes. The EOM-EE-CCSD module yields two negative excitation energies of ~70 kcal mol^{-1} for the biradicaloid ^{1}A' and ^{1}A" states, in line with CCSD convergence to a higher singlet root. These excitation energies agree with the CCSD deviations from the FCIQMC reference (Table 1).

As mentioned before, consistent results are obtained for ^{H}**3b** with all coupled-cluster codes. As expected for a singlet biradicaloid, a large leading t_1 amplitude of 0.39, a $\mathcal{T}_1$ diagnostic of 0.10 and a leading t_2 amplitude of 0.40 signal alert similar to ^{H}**3a** (leading amplitudes indicate associated $\pi_1 \rightarrow \pi_2$ excitations). However, the EOM-EE-CCSD diagnostic calculation yields only positive excitation energies, signaling CCSD convergence to the correct ^{1}A' ground state. As detailed above, the multi-determinantal nature of the biradicaloid wave function of ^{H}**3b** renders higher-order excitation patterns indispensable to achieve reasonable agreement with the (approximate) FCI result. Based on restricted HF reference wave functions, however, we were unable to achieve proper convergence to the lowest singlet state of ^{H}**3a**. We note in passing that the CR-CC(2,3) method, which was recommended, e.g., in earlier work of Cramer *et al.*,[24a,b] yields similarly poor results as standard CCSD(T) and is thus not helpful here.

Motivated by reports of Yamaguchi, Bartlett and Stanton, who have successfully applied broken-symmetry (BS) UHF reference wave functions in coupled-cluster calculations on biradical(oid)s recently,[22] we have investigated the performance of this approach here. The A' and A" broken-symmetry reference determinants were constructed according to Figure 3. The results compiled in Table 3 show at first glance that the BS-UHF wave functions are much better suited references than RHF. BS-CCSD results are already reasonably close to the FCIQMC benchmark and spin-projection according to Yamaguchi[22a,d] achieves agreement better than 1 kcal mol^{-1}. Inclusion of triples in the BS-CCSD(T) and BS-CCSDT calculations does not, however, lead to improved results. It would be interesting to see whether inclusion of higher excitation patterns leads to systematic convergence of results towards the FCIQMC reference values. However, unrestricted BS computations beyond CCSDT were technically not feasible in any of the coupled cluster codes available to us.

These results indicate a pragmatic possibility to assess the intricate electronic structure of biradicaloid states by means of single reference CCSD theory, provided that the coupled-cluster program allows for the use of UHF reference functions in an unrestricted UCCSD framework. Despite these most promising results we would like to convey a note of caution to the interested reader: while non-truncated coupled-cluster theory is strictly orbital invariant[25c] and thus ever higher levels of excitation patterns eventually do converge to the FCI limit for a given basis set, it remains unclear to which extent truncated BS-CC theory profits from error cancellation. While decades of experience have led to detailed insight into the typical error behavior of individual coupled-cluster excitation levels,[7b,77] and the stability of their fortuitous cancellation, no related experience has been reported with BS-CC theory to the best of our knowledge. Further exacting work with this

Table 2. Deviations of CCSD/ano-pVDZ and CCSD(T)/ano-pVDZ energies obtained with the Molpro and MRCC programs referenced to the FCIQMC benchmark in kcal mol^{-1}.

		^{H}**1**	^{H}**3a**		^{H}**3b**	
Program	Method	ΔE_{S-T}	^{1}A'[a]	^{3}A"	^{1}A'	^{3}A'
Molpro	CCSD	8.6	28.0	0.7	21.6	−0.2
	CCSD(T)	5.3	−225.7	0.2	−10.2	0.0
MRCC	CCSD	8.7	70.9	0.6	21.7	−0.4
	CCSD(T)	5.4	68.8	0.9	−9.6	0.5

[a] ^{1}A" state symmetry not accessible with RHF based methods.

Table 3. Computed relative energies for the biradicaloid singlet states of ^{H}**3a** and ^{H}**3b** referenced to separate triplet imidogen and formaldehyde in kcal mol^{-1}; FCIQMC/ano-pVDZ reference data (boldface) and deviations $\Delta\Delta E_{rel}$ obtained with broken-symmetry coupled-cluster variants and the spin-flip equation of motion coupled-cluster approach with the ano-pVDZ basis. For BS-CC also the coupled-cluster $\langle S^2\rangle$ expectation values are provided. Data based on PBE0/def2-TZVPP optimized structures.

Method	^{H}**3a** ^{1}A"	$\langle S^2\rangle$	^{1}A'[b]	$\langle S^2\rangle$	^{H}**3b** ^{1}A'	$\langle S^2\rangle$
FCIQMC	**8.8**		**7.9**		**−2.1**	
BS-CCSD[a]	−0.3 (−3.0)	1.02	−0.8 (−1.2)	1.00	0.5 (2.8)	0.94
BS-CCSD(T)[a]	0.6 (−2.6)	1.09	0.0 (−0.2)	1.00	0.9 (3.1)	0.83
BS-CCSDT[a]	−0.7 (−4.5)	1.34	−0.8 (−1.0)	1.03	−0.4 (1.3)	0.58
EOM-EE-CCSD	2.3		−0.5		–[c]	
EOM-SF-CCSD	−0.2		−0.4		0.9	
EOM-SF-CCSD(T)(a)*	0.0		0.2		0.8	

[a] Broken-symmetry coupled-cluster calculations performed with CFOUR, spin-projection according to Yamaguchi, unprojected values in parentheses. To this end, energies and $\langle S^2\rangle$ expectation values were computed based on a broken-symmetry singlet and a triplet reference determinant. In the BS-CCSDT calculation on the ^{1}A" state of ^{H}**3a** we obtained an $\langle S^2\rangle$ expectation value of 1.34, indicating convergence to the high-spin solution (see below); spin-projection, however, seems to work robustly in this case; [b] At the structure of ^{H}**3a**, the excited ^{1}A" state is nearly degenerate with the biradicaloid ^{1}A' state, which is the ground state of ^{H}**3b** (cf. Figure 3); [c] CCSD converges to the lowest biradicaloid state, which is thus not accessible by means of the EOM approach.

approach would be necessary to judge whether BS-CCSD theory represents a 'Pauling point'[78] with reliable error cancellation behavior or not.

We studied the performance of the EOM-CC ansatz in some more detail. Starting with the singlet CCSD solution, which converged to the higher-lying ^{1}A' excited state for ^{H}**3a**, EOM-EE-CCSD yields a negative excitation energy from which we derive the ^{1}A" state 2.3 kcal mol^{-1} above the FCIQMC benchmark and the biradicaloid ^{1}A' state 0.5 kcal mol^{-1} below the benchmark value. As convergence to the corresponding high-lying ^{1}A' state for ^{H}**3b** could not be achieved, an analogous EOM-EE treatment was not possible for this electromer. As an alternative we investigated the possibility to access the biradicaloid singlet states via a spin-flip excitation from the corresponding high-spin triplet state (see Figure 3). In fact, for ^{H}**3a** the EOM-SF-CCSD approach yields results very close to the FCI reference data (Table 3). While the conventional CCSD solution converges to the correct biradicaloid ^{1}A' state of ^{H}**3b**, but with a substantial error of 21.7 kcal mol^{-1}, the triplet-based EOM-SF-CCSD calculation yields a pleasingly small deviation of merely 0.9 kcal mol^{-1}. Notably, inclusion of perturbative triples in the EOM-SF-CCSD(T)(a)* approach yields exquisite agreement for ^{H}**3a** and brings the error for ^{H}**3b** down to 0.8 kcal mol^{-1} (Table 3).

On the basis of several earlier reports, we also tested the use of Kohn-Sham (KS) reference orbitals for coupled-cluster calculations.[23a–u] We note a visibly more delocalized nature of KS orbitals compared to the HF orbitals (cf. Supporting Information). Employing restricted PBE0 orbitals, CCSD relative energies are quite similar to those obtained with the RHF reference (Tables 1, 2 and 4). For singlet ^{H}**3a** and ^{H}**3b** we observe, however, significantly lower leading t_1 amplitudes of 0.17 and 0.08, respectively, and rather unsuspicious $\mathcal{T}_1$ diagnostics of 0.04 and 0.02, indicating an improved orbital reference quality.[11] Significant – but compared to RHF-CCSD reduced – leading t_2 amplitudes (^{H}**3a**: 0.46 and ^{H}**3b**: 0.36) indicate the expected biradicaloid singlet character of the resulting CCSD wave function and subsequent EOM-EE-CCSD calculations confirm convergence to the lowest root in both cases. Inclusion of perturbative triples still leads to irritatingly large energy contributions but, in stark contrast to the use of an RHF reference, the CCSD(T) results are now in reasonable agreement with the FCIQMC benchmark. Higher excitation patterns result in essentially the same contributions as observed for HF-CC calculations which reflects the fact that coupled cluster theory becomes strictly orbital invariant in the FCI limit. For singlet ^{H}**3a**, however, unproblematic convergence to the lowest root has paramount value. Probably equally important is the fact that the KS orbital reference is obviously much better suited for the assessment of perturbative (T) and (Q) contributions than the HF reference (cf. Table 1). While, clearly, the general validity of this observation needs further careful investigation, it adds a new twist to earlier, more critical conclusions regarding the use of KS orbital references for coupled cluster calculations – in a recent comprehensive assessment Benedek *et al.* noted hardly specific advantages, or even disadvantages using KS-CC vs. HF-CC theories.[23v] We note in passing that no significant effect results from the use of BS-UKS compared to BS-UHF orbital references.

For further scrutiny we tested alternative orbital sets as coupled-cluster references (Table 4). We note, however, very similar results for BP86, OO-MP2, full-valence CASSCF, and Brueckner orbitals with maximum deviations from the benchmark of about 3 kcal mol^{-1} upon inclusion of perturbative triples. Obviously, the near-degeneracy situations present in ^{H}**3a** and ^{H}**3b** profit more from an improved orbital reference, while the strictly degenerate situation in singlet imidogen escapes any single-reference description.

Table 4. Computed relative energies for the singlet and triplet states of ^{H}**3a** and ^{H}**3b** referenced to separate triplet imidogen (^{H}**1**) and formaldehyde and singlet-triplet energy difference for ^{H}**1** in kcal mol^{-1}; FCIQMC/ano-pVDZ reference data (boldface) and deviations $\Delta\Delta E_{rel}$ obtained with several coupled-cluster variants with modified reference orbitals and multi-reference approaches with the ano-pVDZ basis set are given as well. Data based on PBE0/def2-TZVPP optimized structures.

Method	^{H}**1**	^{H}**3a**			^{H}**3b**	
	ΔE_{S-T}	^{1}A''	^{1}A'	^{3}A''	^{1}A'	^{3}A'
FCIQMC	**41.3**	**8.8**	**7.9**	**2.7**	**−2.1**	**1.6**
PBE0-CCSD	8.7	–	27.8	1.2	22.2	−0.2
PBE0-CCSD(T)	5.4	–	−1.8	0.1	1.9	−0.2
PBE0-CCSDT	0.3	–	2.5	0.0	2.9	−0.2
PBE0-CCSDT(Q)	−0.1	–	−2.6	0.0	−1.1	0.0
PBE0-CCSDTQ	0.0	–	−0.3	0.0	0.2	0.0
PBE0-CCSDTQ(P)	0.0	–	−0.6	0.0	−0.2	0.0
BP86-CCSD	8.7	–	27.8	2.0	22.4	0.8
BP86-CCSD(T)	5.3	–	−0.2	−0.1	2.3	0.2
CAS-CCSD	9.9	–	25.5	0.6	21.2	−0.3
CAS-CCSD(T)	6.3	–	0.1	−0.3	2.0	−0.3
OOMP2-CCSD	8.7	–	27.2	1.3	22.6	0.1
OOMP2-CCSD(T)	5.4	–	0.4	−0.1	2.3	−0.2
BD	8.7	–	26.7	0.9	22.0	−0.1
BD(T)	5.4	–	1.5	0.0	2.6	−0.1
CASSCF[a]	4.6	16.4	16.2	17.7	18.2	16.6
CAS-NEVPT2[a]	1.7	−0.4	−0.2	0.1	−0.4	0.4

[a] CASSCF calculations with a full-valence active space.

By design multi-reference methods are well suited for the treatment of biradicaloid systems. While a correct representation of the singlet states of ^{H}**3a** and ^{H}**3b** merely requires a two-electrons in two-orbitals CASSCCF space, the choice of a consistent active space to study chemical reactivity involving fragmentation is far less obvious. For the present case we have thus chosen a full-valence active space and the CASSCF(18,15)-NEVPT2 results deviate by less than 0.5 kcal mol^{-1} from the FCIQMC results. However, such an approach requires clearly prohibitive effort for the assessment of larger molecular systems. Up to this point we thus conclude that KS-reference based coupled cluster provides an intriguingly accurate method, which retains all practical benefits of a single-reference post-HF black box ansatz.

3.2 Basis Set Effects

The calculations reported thus far were performed with the limited ano-pVDZ basis set and we now turn our attention to basis set effects. For the singlet/triplet gap of imidogen we note pleasing convergence of the FCI result towards experiment upon extrapolation to the CBS limit (Table 5). As noted above, the strictly degenerate biradicaloid singlet state of this species represents a notoriously difficult problem for conventional coupled-cluster theory and convergence to the FCI result is observed only upon inclusion of higher order excitations beyond perturbative triples. While the spin-projected BS-CCSD result for singlet imidogen is in remarkable agreement with the benchmark, closer inspection of the unprojected data indicated (probably general) technical intricacies with the BS-CC representation of biradical singlet states arising from strictly degenerate orbitals.[79] We further note that, for this specific species, KS-CC theory provides no advantage over HF-CC theory, both missing the reference value by a substantial margin. The EOM-SF approach, in turn, achieves highly accurate results for singlet imidogen with deviations of 0.4 kcal mol^{-1} for EOM-SF-CCSD and less than 0.1 kcal mol^{-1} for EOM-SF-CCSD(T)(a)* compared to the FCI reference.

For the two triplet states of ^{H}**3a** and ^{H}**3b** we obtained converged results at the CCSDT level, and perturbative quadruples show negligible contributions. As observed before (Table 1), we note unreasonably large individual contributions of perturbative triples and perturbative quadruples for singlet ^{H}**3b**, which persist at the basis set limit and go back to the inadequacy of the RHF reference. As documented for the ano-pVDZ basis set, much higher excitation patterns are needed for a proper assessment of the singlet state. Yet the computational effort for such calculations with larger basis sets is prohibitive.

For both singlet ^{H}**3a** and ^{H}**3b**, spin-projected broken-symmetry CCSD and CCSDT results have shown excellent agreement with FCI above for the smaller ano-pVDZ basis set. Assuming that this quality carries over to the CBS limit, we recommend the BS-CCSDT results as arguably best data available for both species here. We note assuring agreement within 2 kcal mol^{-1} for the EOM-SF-CCSD(T)(a)* singlet energies at the CBS limit. Using KS reference orbitals, the coupled-cluster wave function represents correctly the biradicaloid singlet states and the KS-CCSD(T) result yields reasonable agreement with the reference data, again irritatingly large perturbative triples contributions notwithstanding. In

Table 5. Energies at the extrapolated basis-set limit for singlet and triplet states of ^{H}**3a** and ^{H}**3b** relative to separated triplet imidogen (^{H}**1**) and formaldehyde; singlet-triplet energy difference for ^{H}**1**. All data in kcal mol^{-1}, estimated best results printed in bold face.

Method	^{H}**1**	^{H}**3a**			^{H}**3b**	
	ΔE_{S-T}	^{1}A"	^{1}A'	^{3}A"	^{1}A'	^{3}A'
FCI[a]	**36.4**	–	–	–	–	–
CCSD[a]	46.1	–	65.5[b]	−3.2	13.5	−5.3
CCSD(T)[a]	43.1	–	60.2[b]	−4.1	−17.1	−5.2
CCSDT[a]	37.1	–	63.7[b]	−4.7	−6.4	−5.5
CCSDT(Q)[a]	35.9	–	49.7[b]	**−4.8**	−14.4	**−5.3**
BS-CCSD[c,d]	36.7 (13.5)	1.9 (−0.6)	0.3 (0.1)	–	−8.7 (−6.1)	–
BS-CCSD(T)[c,d]	–[e]	1.8 (−1.1)	0.2 (0.1)	–	−9.4 (−6.8)	–
BS-CCSDT[c,d]	–[e]	**1.0** (−2.3)	**−0.3** (−0.3)	–	**−10.5** (−8.2)	–
EOM-EE-CCSD[d]	–	6.6	3.2	–	–	–
EOM-SF-CCSD[d]	36.8	2.2	1.0	–	−8.0	–
EOM-SF-CCSD(T)(a)*[d]	36.4	2.1	1.2	–	−8.6	–
KS-CCSD[a,f]	46.0	–	31.1	−2.5	14.3	−4.8
KS-CCSD(T)[a,f]	43.1	–	3.1	−5.0	−6.9	−5.9
KS-CCSD(T*)-F12/VTZ[f]	42.4	–	−0.1	−4.6	−8.6	−5.5

[a] Basis-set extrapolation of correlation energies with cc-pVTZ and cc-pVQZ basis sets according to Neese *et al.*[48] (FCI and KS-CC calculations performed with Molpro, BS-CC with CFOUR, EOM-SF-CC with Qcumbre, all other with the MRCC code); [b] convergence to a high-lying ^{1}A' excited state; [c] spin-projected results, non-projected values in parentheses; [d] three point basis-set extrapolation of total energies with cc-pVXZ, X = 2−4, according to Peterson *et al.*[51]; [e] convergence of BS-CC calculations to the triplet solution; [f] calculations with PBE0 orbital reference.

view of the computational effort for the CCSD(T)/VQZ calculations, which becomes quickly prohibitive even for only slightly larger molecular systems, we also tested the use of KS orbitals for CCSD(T*)-F12 calculations. Combined with the VTZ-F12 basis set this method should reach CBS quality while extending the range of accessible molecular sizes. Indeed, the results in Table 5 show pleasing agreement within 2 kcal mol^{-1} with the reference data. We thus recommend this approach as reasonably accurate and computationally most efficient.

3.3 Reaction Pathways of the Minimal Model System

With the freshly benchmarked KS-CC approach at hand we assess the performance of DFT for the imidogen/formaldehyde model system reactivity, covering the hydrogen atom abstraction and nitrogen atom insertion pathways chosen in analogy to the reactivity established for the real metallonitrene pincer complexes (Schemes 1 and 2). Comparison of the PBE0 and KS-CCSD(T*)-F12 results reveals moderate differences of up to 7 kcal mol^{-1} for the hydrogen abstraction path and for the activation barrier for the initial attack of imidogen at the formaldehyde carbon atom via ^{H}**TS2** (Table 6). DFT underestimates both barriers and, somewhat inconsistently, favors C–H abstraction over imidogen attack at the carbon atom. Dramatically larger differences, however, occur further en route towards amide formation. In contrast to expectation[15a,b] the PBE0 hybrid functional does not show the typical overstabilization of triplet over singlet species. On the contrary, in the critical region around intermediate ^{H}**3** the (spin-projected BS) singlet path is dramatically too low compared to the coupled cluster results. As the transition from the triplet potential energy surface near the reactants to the singlet products occurs in this region, a consistent description of both spin states, crucial for any meaningful theoretical assessment of nitrene reactivity, is out of reach for DFT.

Table 6. ΔG_{rel} for the minimal model system in kcal mol^{-1} obtained with the PBE0/def2-TZVPP and the KS-CCSD(T*)-F12/VTZ-F12 method.

Structure	Spin	PBE0	KS-CCSD(T*)-F12[a]
^{H}**1**	1	0.0	0.0
	0	56.7	43.1
^{H}**TS1**	1	9.6	16.5
^{H}**2**	0.5	−7.9	−6.7
^{H}**TS2**	1	10.9	14.6
	0	34.7	50.7
^{H}**3a**	1	−1.8	7.6
	0	3.2	12.0
^{H}**3b**	1	−3.0	6.3
	0	−13.8	3.3
^{H}**TS3**	0	−12.7	0.3
^{H}**4**	0	−97.7	−93.9
^{H}**TS4**	0	0.7	9.7
^{H}**5**	0	−26.1	−23.0

[a] PBE0 reference orbitals; Gibbs free energy contributions taken from the PBE0 calculations.

3.4 Reinvestigation of the Metallonitrene Systems

Finally, we re-evaluated the reaction paths of the palladium and platinum metallonitrene complexes with benzaldehyde. By

Israel Journal of Chemistry

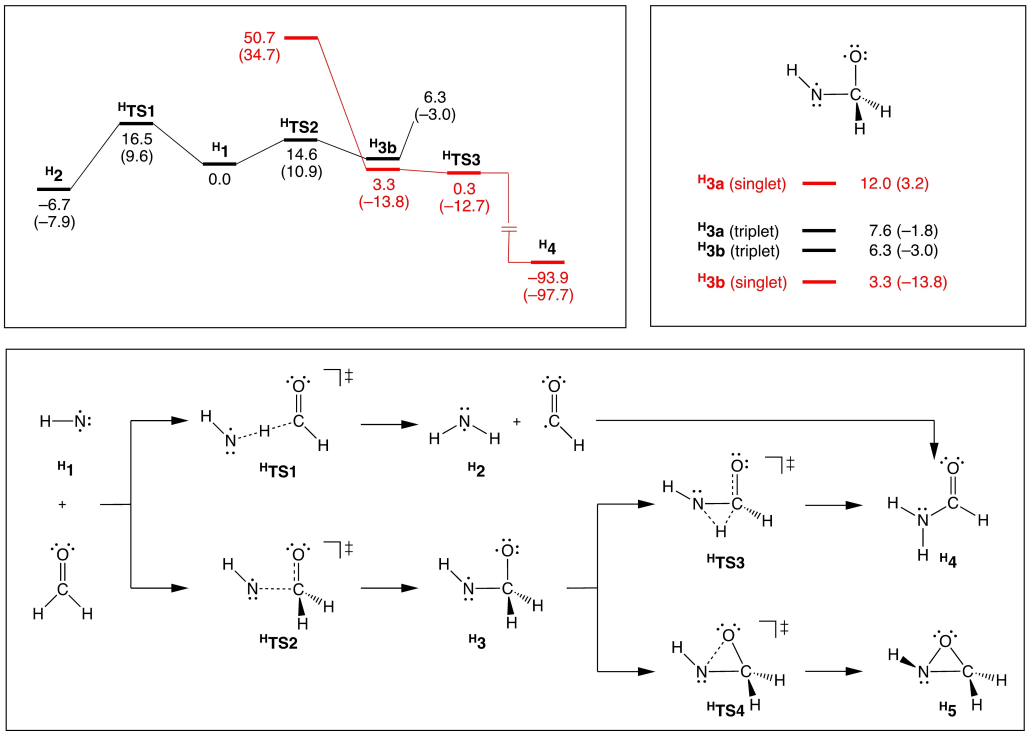

Scheme 2. Schematic representation of the potential energy surface for the reaction of $^{3}\Sigma^{-}$ imidogen with formaldehyde, chosen as minimal model system (top left), and relative electromer energies computed for intermediate ^{H}**3** (top right, ΔG in kcal mol^{-1}, DFT data in parantheses); Lewis-type representation of reaction pathways (bottom, see Table 6 for relative energies of ^{H}**TS4** and ^{H}**5**).

and large, the electronic structure of the metal complexes ^{M}**3** closely resembles that of the minimal model system ^{H}**3**, with only minor metal contributions to spin-densities and key molecular orbitals (exemplarily shown for ^{Pd}**3** in Figure 4, for details of ^{Pt}**3** see Supporting Information). We thus used PBE0-CCSD(T*)-F12/VTZ calculations as high-level method for the model system within the ONIOM approach, while PBE0-D/def2-TZVPP calculations served as low-level method. Scheme 3 shows relative free energies $\Delta G_{\mathrm{ONIOM}}$ computed for stationary points along the pathways studied for both systems. With reference to the detailed breakdown of KS-CC and HF-CC results provided in Tables S13 and S15 we note that the CCSD results for the model system agree within a rather narrow margin regardless of the orbital reference used. As noted above, the (T) contributions for singlet intermediate **3** are unusually large, i.e. in the Pt case 19 kcal mol^{-1} and

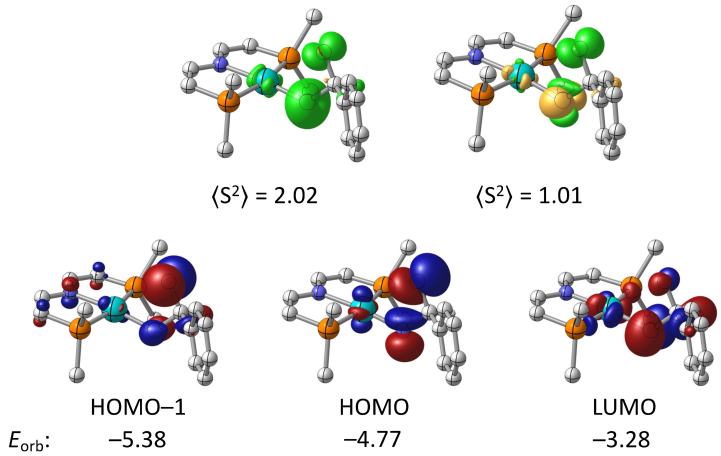

Figure 4. Spin-density plots for the triplet and broken-symmetry singlet solutions of ^{Pd}**3** (top) and PBE0/def2-TZVPP molecular orbitals from an RKS calculation on singlet ^{Pd}**3**. Spin-density isosurfaces at ±0.01 a_0^{-3}, MO isosurfaces at ±0.05 $a_0^{-3/2}$ and orbital energies in eV.

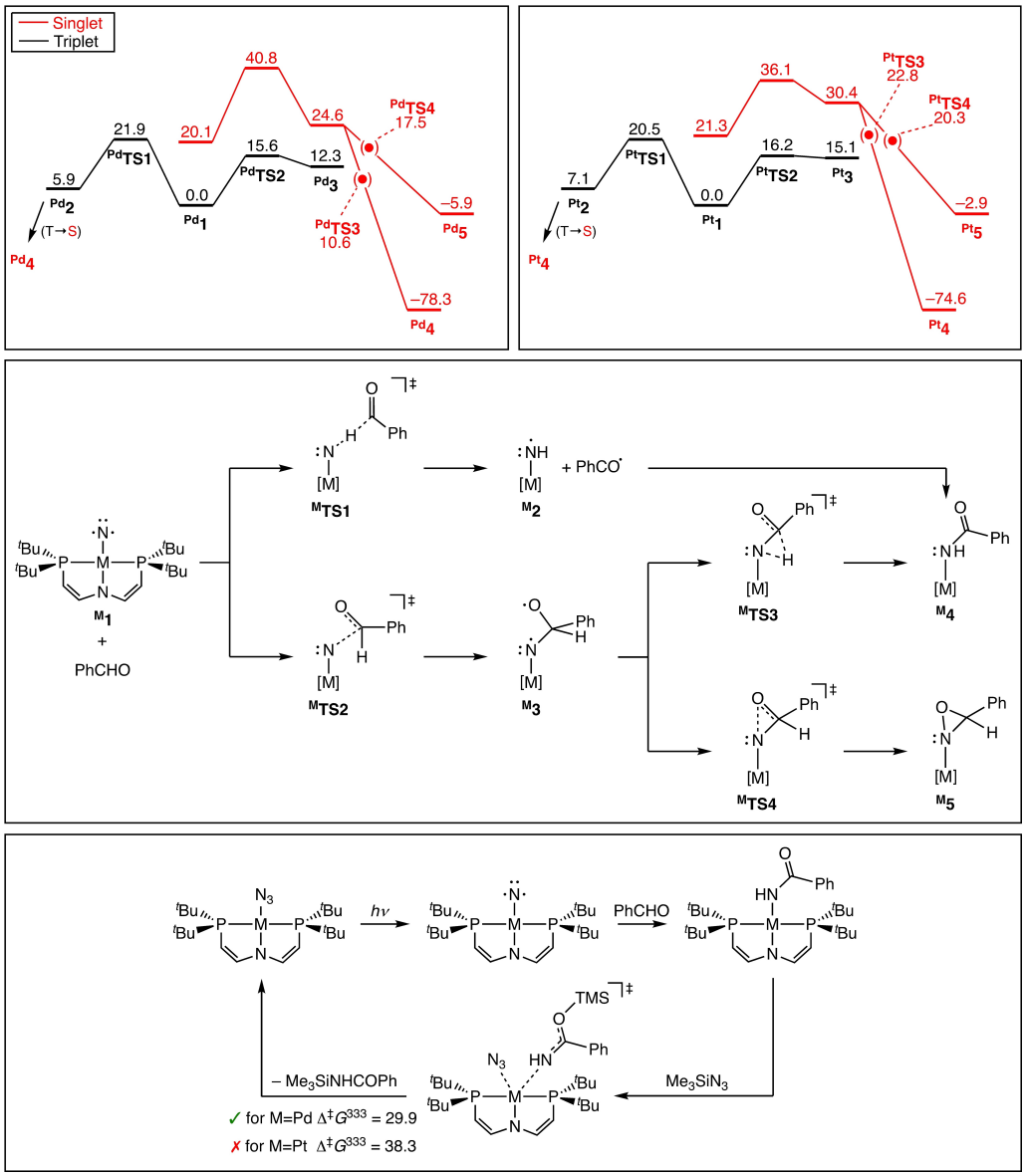

Scheme 3. Schematic representation of the potential energy surface for the reaction of ^{M}**1** with benzaldehyde, M = Pd (left), Pt (right). ONIOM(KS-CCSD(T*)-F12:PBE0-D) results, ΔG in kcal mol^{-1}; Gibbs free energy contributions taken from the PBE0 Hessian calculations on the real system. Singlet surface in red and triplet surface in black; Lewis pictures for reactants, products, intermediates and transition-states (center); catalyst regeneration via transamidation is experimentally accessible only for Pd, but not for Pt (bottom).[5b] Transition states ^{M}**TS3** and ^{M}**TS4**, both localized in BS-DFT geometry optimizations as well-defined stationary points, fall far below the energies of the preceding minima at the ONIOM level.

44 kcal mol^{-1} for KS-CC and HF-CC, respectively, as well as 24 kcal mol^{-1} and enormous 73 kcal mol^{-1} in the Pd case. While the size of these contributions seems to challenge the perturbative nature of the triples ansatz, we scrutinized the KS-CC data obtained for the Pd model system by comparison to BS-CC results: As noted also for the minimal model system above, we find rather small (T) contributions in the BS case, and spin-projection leads to assuring agreement of both BS-CCSD and BS-CCSD(T) with the KS-CCSD(T*)-F12 results (Table 7).

We hence convey the ONIOM data compiled in Scheme 3 as an improved basis for comparison of the Pt and Pd systems. For the Pt system we note a number of significant differences with respect to our earlier publication:[5a] The most obvious difference between the present KS-CC results and the formerly published HF-CC based data is the relative energy of the singlet intermediate ^{Pt}**3**, this species is now assigned a triplet ground state with a well separated singlet. Further, crossing from the triplet to the singlet PES, which evidently occurs en route from the triplet reactants to the singlet reaction products,

Table 7. PBE0-CCSD(T*)-F12/VTZ and basis set extrapolated (BS-)CCSD(T) energies for the singlet and triplet H-truncated ONIOM model system (^{Pd}**3**)^{model}, relative to separate (^{Pd}**1**)^{model} and benzaldehyde (kcal mol^{-1}).

Structure	Spin	$\Delta E^{model}_{KS-CCSD}$	$\Delta E^{model}_{KS-CCSD(T)}$	$\Delta E^{model}_{(BS-)CCSD}$	$\Delta E^{model}_{(BS-)CCSD(T)}$
(^{Pd}**3**)^{model}	1	−2.6	−5.4	−3.8	−5.2
	0	28.5	4.4	5.6 (0.7)[a]	4.4 (−0.7)[a]

[a] Broken-symmetry coupled-cluster calculations performed with ORCA, spin-projection according to Noodleman (Equation 3), unprojected values in parentheses.

is located beyond intermediate ^{Pt}**3**, and not before as previously suggested. More specifically, with relative energies substantially below the preceding minima, the singlet transition states connected with the formation of the products ^{Pt}**4** and ^{Pt}**5** localized at the DFT level do not represent meaningful stationary points anymore at the ONIOM(KS-CC:DFT) level (cf. Supporting Information and Scheme 3). Consequently, both the amide and the oxaziridine products are formed instead in barrierless steps directly from the singlet intermediate ^{Pt}**3**. In ONIOM(KS-CC:DFT) calculations along the intrinsic reaction coordinate connecting ^{Pt}**3** and ^{Pt}**4** we approximated a triplet/singlet crossing point at about 5–9 kcal mol^{-1} above triplet intermediate ^{Pt}**3** (cf. Supporting Information). These results imply a two-state-reactivity scenario,[80] in which the triplet→singlet transition probability determines the rate of amide product formation. The same holds for oxaziridine formation, but this reaction sequence is nearly thermoneutral with respect to the separate reactants; it is thus reversible and does not compete with amide formation.

With differences in detail, the ONIOM results for the Pd system show substantial similarity with the Pt results, both for N-atom transfer and H-abstraction pathways (Scheme 3). This leads us to conclude that the reaction pathways investigated here are not responsible for the experimental observation that the Pt complex shows stoichiometric reactivity, while the Pd complex enables catalytic N-atom transfer. As shown in earlier work,[5b] closure of the catalytic cycle is initiated by transamidation at ^{M}**4** by reaction with, e. g., trimethylsilyl azide (Scheme 3). Product release and catalyst regeneration then involves azide/silylamide ligand exchange. This ligand exchange has a distinctly higher activation barrier in the Pt case ($\Delta^{\ddagger}G^{333K} = 38.3$ kcal mol^{-1}), precluding catalysis at synthetically useful temperatures, while the computed barrier for the Pd case ($\Delta^{\ddagger}G^{333K} = 29.9$ kcal mol^{-1}) is roughly in line with a swift reaction under the experimental conditions (T = 333 K, DFT data as reported in Ref. [5b]).

4. Conclusions

In summary, we have shown that the biradicaloid nature of singlet intermediates ^{M}**3** gives rise to the severe problems of CCSD(T) theory we had encountered in earlier quantum-chemical reactivity studies of Pd(II) and Pt(II) metallonitrene systems. For detailed analysis we devised a minimal model system that mimics the problematic electronic structure of the full transition metal complexes. For this model we established reliable reference energies based on approximate full configuration interaction theory and we studied the performance of single-reference coupled-cluster theory up to the CCSDTQ(P) excitation level. We found that in some cases RHF-based CCSD(T) theory applied to biradicaloid systems showed a particularly poor performance with devastating errors in perturbative triples contributions exceeding 220 kcal mol^{-1}. In other cases, the coupled-cluster wave function converged to excited states, with errors up to 70 kcal mol^{-1}; EOM-CC theory was used as a convenient diagnostic to identify such situations.

We investigated the influence of various alternative reference wave functions on the quality of results. We found that EOM-SF-CCSD(T)(a)* theory, ground-state KS-CCSD(T) theory employing Kohn-Sham reference orbitals, as well as broken-symmetry BS-CCSD(T) theory gave particularly good agreement with the reference data, with the latter two even maintaining the cost of 'gold-standard' coupled-cluster theory. For the BS-CC approach, spin-projection turned out to be critical for accurate results, while increasing the coupled-cluster expansion beyond BS-CCSD showed only minor effects. KS-CCSD results, on the other hand, showed no particular accuracy advantage over HF-CCSD results apart from the fact that convergence to highly excited singlet states, which plagued the latter approach, was not observed. Perturbative triples, however, profit substantially from the use of KS reference orbitals. The KS-CCSD(T) approach has shown no significant downsides compared to conventional HF-CCSD(T), it provides superior performance in problematic cases such as studied here, and it is easy to use with most quantum-chemical programs.

Finally, we applied the KS-CCSD(T*)-F12b variant as high-level part of an ONIOM(KS-CC:DFT) scheme to reinvestigate the N-atom transfer reactivity of Pt and Pd metallonitrene systems with benzaldehyde. The revised reaction path energetics exhibit substantial differences to ONIOM(HF-CC:DFT) results published earlier only in the region around intermediates ^{M}**3**. By and large, the revised set of results demonstrates far reaching similarities for the N-atom transfer reactivity of the Pd and Pt systems. Marked differences between the two systems exist, however, for the energetics of the subsequent transamidation, which is critical for catalyst regeneration. This is an important finding with implications for related experimental work.

Acknowledgements

George Booth (King's College London), Oskar Weser, and Ali Alavi (Max-Planck-Institut für Festkörperforschung Stuttgart) are acknowledged for most helpful technical advice with the FCIQMC computations. We gratefully acknowledge stimulating discussions with John Stanton (University of Florida). M.U. thanks the Deutsche Forschungsgemeinschaft (DFG) for funding through Emmy-Noether project RO 5688/1. St.St. acknowledges support by the Deutsche Forschungsgemeinschaft (DFG) grant number STO 1239/1-1 and within project B5 of the TRR 146 (Project No. 233 630 050). Quantum-chemical calculations were performed at the Center for Scientific Computing (CSC) Frankfurt on the Goethe-HLR computer cluster. Open Access funding enabled and organized by Projekt DEAL.

Data Availability Statement

The data that support the findings of this study are available in the supplementary material of this article.

References

[1] a) G. Dequirez, V. Pons, P. Dauban, *Angew. Chem. Int. Ed.* **2012**, *51*, 7384–7395; b) D. E. Falvey, A. D. Gudmundsdottir, *Nitrenes and Nitrenium Ions*, Wiley, New York, **2013**; c) C. Wentrup, *Angew. Chem. Int. Ed.* **2018**, *57*, 11508–11521.

[2] a) S.-M. Au, J.-S. Huang, W.-Y. Yu, W.-H. Fung, C.-M. Che, *J. Am. Chem. Soc.* **1999**, *121*, 9120–9132; b) K. W. Fiori, J. Du Bois, *J. Am. Chem. Soc.* **2007**, *129*, 562–568; c) Y. M. Badiei, A. Dinescu, X. Dai, R. M. Palomino, F. W. Heinemann, T. R. Cundari, T. H. Warren, *Angew. Chem. Int. Ed.* **2008**, *47*, 9961–9964; d) E. R. King, E. T. Hennessy, T. A. Betley, *J. Am. Chem. Soc.* **2011**, *133*, 4917–4923; e) V. Lyaskovskyy, A. I. O. Suarez, H. Lu, H. Jiang, X. P. Zhang, B. de Bruin, *J. Am. Chem. Soc.* **2011**, *133*, 12264–12273; f) M. E. Harvey, D. G. Musaev, J. Du Bois, *J. Am. Chem. Soc.* **2011**, *133*, 17207–17216; g) S. Kundu, E. Miceli, E. Farquhar, F. F. Pfaff, U. Kuhlmann, P. Hildebrandt, B. Braun, C. Greco, K. Ray, *J. Am. Chem. Soc.* **2012**, *134*, 14710–14713; h) S. M. Paradine, J. R. Griffin, J. Zhao, A. L. Petronico, S. M. Miller, M. C. White, *Nat. Chem.* **2015**, *7*, 987–994; i) P. F. Kuijpers, J. I. van der Vlugt, S. Schneider, B. de Bruin, *Chem. Eur. J.* **2017**, *23*, 13819–13829; j) S. Hong, K. D. Sutherlin, A. K. Vardhaman, J. J. Yan, S. Park, Y.-M. Lee, S. Jang, X. Lu, T. Ohta, T. Ogura, E. I. Solomon, W. Nam, *J. Am. Chem. Soc.* **2017**, *139*, 8800–8803; k) C. Weatherly, J. M. Alderson, J. F. Berry, J. E. Hein, J. M. Schomaker, *Organometallics* **2017**, *36*, 1649–1661; l) K. M. Carsch, I. M. DiMucci, D. A. Iovan, A. Li, S.-L. Zheng, C. J. Titus, S. J. Lee, K. D. Irwin, D. Nordlund, K. M. Lancaster, T. A. Betley, *Science* **2019**, *365*, 1138–1143; m) A. Grünwald, S. S. Anjana, D. Munz, *Eur. J. Inorg. Chem.* **2021**, *2021*, 4147–4166; n) Y.-C. Wang, X.-J. Lai, K. Huang, S. Yadav, G. Qiu, L. Zhang, H. Zhou, *Org. Chem. Front.* **2021**, *8*, 1677–1693; o) A. Reckziegel, M. Kour, B. Battistella, S. Mebs, K. Beuthert, R. Berger, C. G. Werncke, *Angew. Chem. Int. Ed.* **2021**, *60*, 15376–15380; p) S. Reith, S. Demeshko, B. Battistella, A. Reckziegel, C. Schneider, A. Stoy, C. Lichtenberg, F. Meyer, D. Munz, C. G. Werncke, *Chem. Sci.* **2022**, *13*, 7907–7913.

[3] a) B. Askevold, J. T. Nieto, S. Tussupbayev, M. Diefenbach, E. Herdtweck, M. C. Holthausen, S. Schneider, *Nat. Chem.* **2011**, *3*, 532–537; b) J. Abbenseth, M. Finger, C. Würtele, M. Kasanmascheff, S. Schneider, *Inorg. Chem.* **2016**, *3*, 469–477; c) G. A. Silantyev, M. Förster, B. Schluschaß, J. Abbenseth, C. Würtele, C. Volkmann, M. C. Holthausen, S. Schneider, *Angew. Chem. Int. Ed.* **2017**, *56*, 5872–5876; d) S. J. K. Forrest, B. Schluschaß, E. Y. Yuzik-Klimova, S. Schneider, *Chem. Rev.* **2021**, *121*, 6522–6587; e) L. Alig, K. A. Eisenlohr, Y. Zelenkova, S. Rosendahl, R. Herbst-Irmer, S. Demeshko, M. C. Holthausen, S. Schneider, *Angew. Chem. Int. Ed.* **2022**, *61*, e202113340; f) J. Abbenseth, J.-P. H. Oudsen, B. Venderbosch, S. Demeshko, M. Finger, C. Herwig, C. Würtele, M. C. Holthausen, C. Limberg, M. Tromp, S. Schneider, *Inorg. Chem.* **2020**, *59*, 14367–14375; g) M. Kinauer, M. Diefenbach, H. Bamberger, S. Demeshko, E. J. Reijerse, C. Volkmann, C. Würtele, J. van Slageren, B. de Bruin, M. C. Holthausen, S. Schneider, *Chem. Sci.* **2018**, *9*, 4325–4332.

[4] a) C. C. Hojilla Atienza, A. C. Bowman, E. Lobkovsky, P. J. Chirik, *J. Am. Chem. Soc.* **2010**, *132*, 16343–16345; b) J. Schöffel, N. Šušnjar, S. Nückel, D. Sieh, P. Burger, *Eur. J. Inorg. Chem.* **2010**, *2010*, 4911–4915; c) M. G. Scheibel, B. Askevold, F. W. Heinemann, E. J. Reijerse, B. de Bruin, S. Schneider, *Nat. Chem.* **2012**, *4*, 552–558; d) V. Vreeken, M. A. Siegler, B. de Bruin, J. N. H. Reek, M. Lutz, J. I. van der Vlugt, *Angew. Chem. Int. Ed.* **2015**, *54*, 7055–7059; e) M. G. Scheibel, J. Abbenseth, M. Kinauer, F. W. Heinemann, C. Würtele, B. de Bruin, S. Schneider, *Inorg. Chem.* **2015**, *54*, 9290–9302; f) V. Vreeken, L. Baij, B. de Bruin, M. A. Siegler, J. I. van der Vlugt, *Dalton Trans.* **2017**, *46*, 7145–7149; g) Z. Sun, O. A. Hull, T. R. Cundari, *Inorg. Chem.* **2018**, *57*, 6807–6815; h) D. C. Alamo, T. R. Cundari, *Inorg. Chem.* **2021**, *60*, 12299–12308.

[5] a) J. Sun, J. Abbenseth, H. Verplancke, M. Diefenbach, B. de Bruin, D. Hunger, C. Würtele, J. van Slageren, M. C. Holthausen, S. Schneider, *Nat. Chem.* **2020**, *12*, 1054–1059; b) T. Schmidt-Räntsch, H. Verplancke, J. N. Lienert, S. Demeshko, M. Otte, G. P. Van Trieste 3rd, K. A. Reid, J. H. Reibenspies, D. C. Powers, M. C. Holthausen, S. Schneider, *Angew. Chem. Int. Ed.* **2022**, *61*, e202115626.

[6] K. Raghavachari, G. W. Trucks, J. A. Pople, M. Head-Gordon, *Chem. Phys. Lett.* **1989**, *157*, 479–483.

[7] a) J. F. Stanton, *Chem. Phys. Lett.* **1997**, *281*, 130–134; b) J. M. L. Martin, *Isr. J. Chem.* **2022**, *62*, e202100111.

[8] a) R. O. Ramabhadran, K. Raghavachari, *Acc. Chem. Res.* **2014**, *47*, 3596–3604; b) R. O. Ramabhadran, K. Raghavachari, *J. Chem. Theory Comput.* **2013**, *9*, 3986–3994; c) M. A. Collins, R. P. A. Bettens, *Chem. Rev.* **2015**, *115*, 5607–5642; d) K. Raghavachari, A. Saha, *Chem. Rev.* **2015**, *115*, 5643–5677.

[9] a) Q. Ma, H.-J. Werner, *WIREs Comput. Mol. Sci.* **2018**, *8*, e1371; b) F. Neese, A. Hansen, D. G. Liakos, *J. Chem. Phys.* **2009**, *131*, 064103; c) C. Riplinger, F. Neese, *J. Chem. Phys.* **2013**, *138*, 034106; d) Y. Guo, C. Riplinger, U. Becker, D. G. Liakos, Y. Minenkov, L. Cavallo, F. Neese, *J. Chem. Phys.* **2018**, *148*, 011101; e) Z. Rolik, M. Kállay, *J. Chem. Phys.* **2011**, *135*, 104111; f) P. R. Nagy, M. Kállay, *J. Chem. Theory Comput.* **2019**, *15*, 5275–5298.

[10] a) J. A. Keith, V. Vassilev-Galindo, B. Cheng, S. Chmiela, M. Gastegger, K.-R. Müller, A. Tkatchenko, *Chem. Rev.* **2021**, *121*, 9816–9872; b) G. M. Jones, P. D. V. S. Pathirage, K. D. Vogiatzis, in *Quantum Chemistry in the Age of Machine Learning* (Ed.: P. O. Dral), Elsevier, **2023**, pp. 509–529.

[11] J. D. Watts, R. J. Bartlett, *Int. J. Quantum Chem.* **1994**, *52*, 195–203.

[12] a) J. Abbenseth, M. Diefenbach, S. C. Bete, C. Würtele, C. Volkmann, S. Demeshko, M. C. Holthausen, S. Schneider, *Chem. Commun.* **2017**, *53*, 5511–5514; b) D. Delony, M. Kinauer, M. Diefenbach, S. Demeshko, C. Würtele, M. C. Holthausen, S. Schneider, *Angew. Chem. Int. Ed.* **2019**, *58*, 10971–10974; c) J. Sun, H. Verplancke, J. I. Schweizer, M. Diefenbach, C. Würtele, M. Otte, I. Tkach, C. Herwig, C. Limberg, S. Demeshko, M. C. Holthausen, S. Schneider, *Chem* **2021**, *7*, 1952–1962.

[13] L. W. Chung, W. M. C. Sameera, R. Ramozzi, A. J. Page, M. Hatanaka, G. P. Petrova, T. V. Harris, X. Li, Z. Ke, F. Liu, H.-B. Li, L. Ding, K. Morokuma, *Chem. Rev.* **2015**, *115*, 5678–5796.

[14] T. B. Adler, G. Knizia, H. J. Werner, *J. Chem. Phys.* **2007**, *127*, 221106.

[15] a) S. M. Tekarli, T. G. Williams, T. R. Cundari, *J. Chem. Theory Comput.* **2009**, *5*, 2959–2966; b) T. R. Cundari, A. Dinescu, A. B. Kazi, *Inorg. Chem.* **2008**, *47*, 10067–10072; c) S. Vyas, A. H. Winter, C. M. Hadad, in *Nitrenes and Nitrenium Ions* (Eds.: D. E. Falvey, A. D. Gudmundsdottir), Wiley, New York, **2013**, pp. 33–76.

[16] a) R. Lindh, T. J. Lee, A. Bernhardsson, B. J. Persson, G. Karlstroem, *J. Am. Chem. Soc.* **1995**, *117*, 7186–7194; b) E. Kraka, D. Cremer, G. Bucher, H. Wandel, W. Sander, *Chem. Phys. Lett.* **1997**, *268*, 313–320; c) C. J. Cramer, J. J. Nash, R. R. Squires, *Chem. Phys. Lett.* **1997**, *277*, 311–320; d) C. J. Cramer, *J. Am. Chem. Soc.* **1998**, *120*, 6261–6269; e) D. G. Liakos, F. Neese, *J. Chem. Theory Comput.* **2011**, *7*, 1511–1523; f) L. Sandhiya, H. Zipse, *J. Comput. Chem.* **2017**, *38*, 2186–2192.

[17] a) F. Neese, W. Ames, G. Christian, M. Kampa, D. G. Liakos, D. A. Pantazis, M. Roemelt, P. Surawatanawong, S. Ye, in *Adv. Inorg. Chem., Vol. 62* (Eds.: R. van Eldik, J. Harvey), Academic Press, **2010**, pp. 301–349; b) D. I. Lyakh, M. Musiał, V. F. Lotrich, R. J. Bartlett, *Chem. Rev.* **2012**, *112*, 182–243; c) K. R. Yang, A. Jalan, W. H. Green, D. G. Truhlar, *J. Chem. Theory Comput.* **2013**, *9*, 418–431; d) J. P. Malrieu, R. Caballol, C. J. Calzado, C. de Graaf, N. Guihery, *Chem. Rev.* **2014**, *114*, 429–492; e) C. Sousa, C. de Graaf, in *Spin states in biochemistry and inorganic chemistry* (Eds.: M. Swart, M. Costas), Wiley, Chichester, **2016**; f) D. J. Coughtrie, R. Giereth, D. Kats, H.-J. Werner, A. Köhn, *J. Chem. Theory Comput.* **2018**, *14*, 693–709; g) M. Roemelt, D. A. Pantazis, *Adv. Theory Simul.* **2019**, *2*, 1800201.

[18] I. Shavitt, R. J. Bartlett, *Many-Body Methods in Chemistry and Physics: MBPT and Coupled-Cluster Theory*, Cambridge University Press, Cambridge, **2009**.

[19] a) A. I. Krylov, *Chem. Phys. Lett.* **2001**, *338*, 375–384; b) L. V. Slipchenko, A. I. Krylov, *J. Chem. Phys.* **2002**, *117*, 4694–4708; c) A. I. Krylov, *Acc. Chem. Res.* **2006**, *39*, 83–91.

[20] D. A. Matthews, J. F. Stanton, *J. Chem. Phys.* **2016**, *145*, 124102.

[21] a) L. Noodleman, *J. Chem. Phys.* **1981**, *74*, 5737–5743; b) L. Noodleman, E. R. Davidson, *Chem. Phys.* **1986**, *109*, 131–143; c) K. Yamaguchi, Y. Takahara, T. Fueno, in *Applied Quantum Chemistry* (Eds.: V. H. Smith Jr., H. F. Schaefer III, K. Morokuma), Reidel, Dordrecht, **1986**, p. 155; d) S. Yamanaka, T. Kawakami, H. Nagao, K. Yamaguchi, *Chem. Phys. Lett.* **1994**, *231*, 25–33; e) A. Bencini, F. Totti, C. A. Daul, K. Doclo, P. Fantucci, V. Barone, *Inorg. Chem.* **1997**, *36*, 5022–5030; f) R. Caballol, O. Castell, F. Illas, I. de P. R. Moreira, J. P. Malrieu, *J. Phys. Chem. A* **1997**, *101*, 7860–7866; g) F. Illas, I. P. R. Moreira, C. de Graaf, V. Barone, *Theor. Chem. Acc.* **2000**, *104*, 265–272; h) J. Gräfenstein, E. Kraka, M. Filatov, D. Cremer, *Int. J. Mol. Sci.* **2002**, *3*, 360–394; i) D. Cremer, M. Filatov, V. Polo, E. Kraka, S. Shaik, *Int. J. Mol. Sci.* **2002**, *3*, 604–638; j) I. Ciofini, C. A. Daul, *Coord. Chem. Rev.* **2003**, *238–239*, 187–209; k) E. Ruiz, A. Rodríguez-Fortea, J. Cano, S. Alvarez, P. Alemany, *J. Comput. Chem.* **2003**, *24*, 982–989; l) F. Neese, *J. Phys. Chem. Solids* **2004**, *65*, 781–785; m) E. Ruiz, S. Alvarez, J. Cano, V. Polo, *J. Chem. Phys.* **2005**, *123*, 164110; n) C. Adamo, V. Barone, A. Bencini, R. Broer, M. Filatov, N. M. Harrison, F. Illas, J. P. Malrieu, I. d. P. R. Moreira, *J. Chem. Phys.* **2006**, *124*, 107101; o) E. Ruiz, J. Cano, S. Alvarez, V. Polo, *J. Chem. Phys.* **2006**, *124*, 107102; p) F. Neese, *Coord. Chem. Rev.* **2009**, *253*, 526–563; q) Y. Kitagawa, T. Saito, K. Yamaguchi, in *Symmetry (Group Theory) and Mathematical Treatment in Chemistry* (Ed.: T. Akitsu), IntechOpen, **2018**; r) D. A. Pantazis, *Inorganics* **2019**, *7*, 57.

[22] a) T. Saito, N. Yasuda, Y. Kataoka, Y. Nakanishi, Y. Kitagawa, T. Kawakami, S. Yamanaka, M. Okumura, K. Yamaguchi, *J. Phys. Chem. A* **2011**, *115*, 5625–5631; b) T. Saito, A. Ito, T. Watanabe, T. Kawakami, M. Okumura, K. Yamaguchi, *Chem. Phys. Lett.* **2012**, *542*, 19–25; c) J. T. Margraf, A. Perera, J. J. Lutz, R. J. Bartlett, *J. Chem. Phys.* **2017**, *147*, 184101; d) H. F. Schurkus, G. K. Chan, D. T. Chen, H. P. Cheng, J. F. Stanton, *J. Chem. Phys.* **2020**, *152*, 234115.

[23] a) M. Warken, *Chem. Phys. Lett.* **1995**, *237*, 256–263; b) P. Bouř, *Chem. Phys. Lett.* **2001**, *345*, 331–337; c) L. Veseth, *J. Chem. Phys.* **2001**, *114*, 8789–8795; d) T. Hupp, B. Engels, F. Della Sala, A. Görling, *Chem. Phys. Lett.* **2002**, *360*, 175–181; e) T. Hupp, B. Engels, F. Della Sala, A. Görling, *Z. Phys. Chem.* **2003**, *217*, 133–159; f) T. Hupp, B. Engels, A. Görling, *J. Chem. Phys.* **2003**, *119*, 11591–11601; g) G. J. O. Beran, S. R. Gwaltney, M. Head-Gordon, *Phys. Chem. Chem. Phys.* **2003**, *5*, 2488–2493; h) J. N. Harvey, M. Aschi, *Faraday Discuss.* **2003**, *124*, 129–143; discussion 145–153, 453–455; i) F. Neese, D. G. Liakos, S. Ye, *J. Biol. Inorg. Chem.* **2011**, *16*, 821–829; j) J. N. Harvey, D. P. Tew, *Int. J. Mass Spectrom.* **2013**, *354–355*, 263–270; k) A. S. Petit, R. C. R. Pennifold, J. N. Harvey, *Inorg. Chem.* **2014**, *53*, 6473–6481; l) Z. Fang, Z. Lee, K. A. Peterson, D. A. Dixon, *J. Chem. Theory Comput.* **2016**, *12*, 3583–3592; m) Z. Fang, M. Vasiliu, K. A. Peterson, D. A. Dixon, *J. Chem. Theory Comput.* **2017**, *13*, 1057–1066; n) M. Radon, *Phys. Chem. Chem. Phys.* **2019**, *21*, 4854–4870; o) S. E. Neale, D. A. Pantazis, S. A. Macgregor, *Dalton Trans.* **2020**, *49*, 6478–6487; p) A. Rettig, D. Hait, L. W. Bertels, M. Head-Gordon, *J. Chem. Theory Comput.* **2020**, *16*, 7473–7489; q) L. W. Bertels, J. Lee, M. Head-Gordon, *J. Chem. Theory Comput.* **2021**, *17*, 742–755; r) M. Drosou, C. A. Mitsopoulou, D. A. Pantazis, *Polyhedron* **2021**, *208*; s) S. Mallick, P. K. Rai, P. Kumar, *Comput. Theor. Chem.* **2021**, *1202*, 113326; t) G. Drabik, J. Szklarzewicz, M. Radon, *Phys. Chem. Chem. Phys.* **2021**, *23*, 151–172; u) A. Stanczak, J. Chalupsky, L. Rulisek, M. Straka, *ChemPhysChem* **2022**, *23*, e202200076; v) Z. Benedek, P. Timar, T. Szilvasi, G. Barcza, *J. Comput. Chem.* **2022**, *43*, 2103–2120.

[24] a) C. J. Cramer, M. Włoch, P. Piecuch, C. Puzzarini, L. Gagliardi, *J. Phys. Chem. A* **2006**, *110*, 1991–2004; b) C. J. Cramer, M. Włoch, P. Piecuch, C. Puzzarini, L. Gagliardi, *J. Phys. Chem. A* **2007**, *111*, 4871–4871; c) C. J. Cramer, A. Kinal, M. Włoch, P. Piecuch, L. Gagliardi, *J. Phys. Chem. A* **2006**, *110*, 11557–11568; d) C. J. Cramer, J. R. Gour, A. Kinal, M. Włoch, P. Piecuch, A. R. Moughal Shahi, L. Gagliardi, *J. Phys. Chem. A* **2008**, *112*, 3754–3767; e) K. Samanta, C. A. Jiménez-Hoyos, G. E. Scuseria, *J. Chem. Theory Comput.* **2012**, *8*, 4944–4949; f) A. Stańczak, J. Chalupský, L. Rulíšek, M. Straka, *ChemPhysChem* **2022**, *23*, e202200076.

[25] a) T. J. Lee, G. E. Scuseria, in *Quantum Mechanical Electronic Structure Calculations with Chemical Accuracy* (Ed.: S. R. Langhoff), Springer, Dordrecht, **1995**, pp. 47–108; b) T. Hel-

gaker, P. Jørgensen, J. Olsen, *Molecular Electronic-Structure Theory*, Wiley, Chichester, **2000**; c) R. J. Bartlett, M. Musiał, *Rev. Mod. Phys.* **2007**, *79*, 291–352.

[26] M. J. Frisch, G. W. Trucks, H. B. Schlegel, G. E. Scuseria, M. A. Robb, J. R. Cheeseman, G. Scalmani, V. Barone, G. A. Petersson, H. Nakatsuji, X. Li, M. Caricato, A. V. Marenich, J. Bloino, B. G. Janesko, R. Gomperts, B. Mennucci, H. P. Hratchian, J. V. Ortiz, A. F. Izmaylov, J. L. Sonnenberg, D. Williams-Young, F. Ding, F. Lipparini, F. Egidi, J. Goings, B. Peng, A. Petrone, T. Henderson, D. Ranasinghe, V. G. Zakrzewski, J. Gao, N. Rega, G. Zheng, W. Liang, M. Hada, M. Ehara, K. Toyota, R. Fukuda, J. Hasegawa, M. Ishida, T. Nakajima, Y. Honda, O. Kitao, H. Nakai, T. Vreven, K. Throssell, J. A. Montgomery, J. E. Peralta, F. Ogliaro, M. J. Bearpark, J. J. Heyd, E. N. Brothers, K. N. Kudin, V. N. Staroverov, T. A. Keith, R. Kobayashi, J. Normand, K. Raghavachari, A. P. Rendell, J. C. Burant, S. S. Iyengar, J. Tomasi, M. Cossi, J. M. Millam, M. Klene, C. Adamo, R. Cammi, J. W. Ochterski, R. L. Martin, K. Morokuma, O. Farkas, J. B. Foresman, D. J. Fox, Gaussian 16, Revision C.01 Gaussian, Inc., Wallingford CT, **2016**.

[27] a) J. P. Perdew, M. Ernzerhof, K. Burke, *J. Chem. Phys.* **1996**, *105*, 9982–9985; b) C. Adamo, V. Barone, *J. Chem. Phys.* **1999**, *110*, 6158–6170.

[28] a) S. Grimme, J. Antony, S. Ehrlich, H. Krieg, *J. Chem. Phys.* **2010**, *132*, 154104; b) A. D. Becke, E. R. Johnson, *J. Chem. Phys.* **2005**, *123*, 154101; c) E. R. Johnson, A. D. Becke, *J. Chem. Phys.* **2005**, *123*, 24101; d) E. R. Johnson, A. D. Becke, *J. Chem. Phys.* **2006**, *124*, 174104; e) S. Grimme, S. Ehrlich, L. Goerigk, *J. Comput. Chem.* **2011**, *32*, 1456–1465.

[29] F. Weigend, R. Ahlrichs, *Phys. Chem. Chem. Phys.* **2005**, *7*, 3297–3305.

[30] D. Andrae, U. Häußermann, M. Dolg, H. Stoll, H. Preuß, *Theor. Chim. Acta* **1990**, *77*, 123–141.

[31] a) M. Mitoraj, A. Michalak, *Organometallics* **2007**, *26*, 6576–6580; b) M. P. Mitoraj, A. Michalak, T. Ziegler, *J. Chem. Theory Comput.* **2009**, *5*, 962–975.

[32] G. te Velde, F. M. Bickelhaupt, E. J. Baerends, C. Fonseca Guerra, S. J. A. van Gisbergen, J. G. Snijders, T. Ziegler, *J. Comput. Chem.* **2001**, *22*, 931–967.

[33] E. Van Lenthe, E. J. Baerends, *J. Comput. Chem.* **2003**, *24*, 1142–1156.

[34] a) F. Neese, *WIREs Comput. Mol. Sci.* **2017**, *8*, e1327; b) F. Neese, F. Wennmohs, U. Becker, C. Riplinger, *J. Chem. Phys.* **2020**, *152*, 224108.

[35] a) H.-J. Werner, P. J. Knowles, G. Knizia, F. R. Manby, M. Schütz, *WIREs Comput. Mol. Sci.* **2012**, *2*, 242–253; b) H.-J. Werner, P. J. Knowles, G. Knizia, F. R. Manby, M. Schütz, P. Celani, W. Györffy, D. Kats, T. Korona, R. Lindh, A. Mitrushenkov, G. Rauhut, K. R. Shamasundar, T. B. Adler, R. D. Amos, A. Bernhardsson, A. Berning, D. L. Cooper, M. J. O. Deegan, A. J. Dobbyn, F. Eckert, E. Goll, C. Hampel, A. Hesselmann, G. Hetzer, T. Hrenar, G. Jansen, C. Köppl, Y. Liu, A. W. Lloyd, R. A. Mata, A. J. May, S. J. McNicholas, W. Meyer, M. E. Mura, A. Nicklass, D. P. O'Neill, P. Palmieri, D. Peng, K. Pflüger, R. Pitzer, M. Reiher, T. Shiozaki, H. Stoll, A. J. Stone, R. Tarroni, T. Thorsteinsson, M. Wang, MOLPRO, version 2015.1, a package of ab initio programs, see http://www.molpro.net, **2015**.

[36] a) D. A. Matthews, L. Cheng, M. E. Harding, F. Lipparini, S. Stopkowicz, T. C. Jagau, P. G. Szalay, J. Gauss, J. F. Stanton, *J. Chem. Phys.* **2020**, *152*, 214108; b) J. F. Stanton, J. Gauss, L. Cheng, M. E. Harding, D. A. Matthews, P. G. Szalay, A. A. Auer, A. Asthana, R. J. Bartlett, U. Benedikt, C. Berger, D. E. Bernholdt, S. Blaschke, Y. J. Bomble, S. Burger, O. Christiansen, D. Datta, F. Engel, R. Faber, J. Greiner, M. Heckert, O. Heun, M. Hilgenberg, C. Huber, T.-C. Jagau, D. Jonsson, J. Jusélius, T. Kirsch, K. Klein, G. M. Kopper, W. J. Lauderdale, F. Lipparini, J. Liu, T. Metzroth, L. A. Mück, T. Nottoli, D. P. O'Neill, D. R. Price, E. Prochnow, C. Puzzarini, K. Ruud, F. Schiffmann, W. Schwalbach, C. Simmons, S. Stopkowicz, A. Tajti, J. Vázquez, F. Wang, J. D. Watts, CFOUR, Coupled-Cluster techniques for Computational Chemistry Version 2.1, and the integral packages MOLECULE (J. Almlöf and P. R. Taylor), PROPS (P. R. Taylor), ABACUS (T. Helgaker, H. J. Aa. Jensen, P. Jørgensen, and J. Olsen), and ECP routines by A. V. Mitin and C. van Wüllen. For the current version, see http://www.cfour.de, **2019**; c) M. E. Harding, T. Metzroth, J. Gauss, A. A. Auer, *J. Chem. Theory Comput.* **2008**, *4*, 64–74.

[37] a) F. Hampe, S. Stopkowicz, N. Groß, M.-P. Kitsaras, L. Grazioli, S. Blaschke, Qcumbre, Quantum Chemical Utility enabling Magnetic-field dependent investigations Benefitting from Rigorous Electron-correlation treatment., **2022**; b) F. Hampe, S. Stopkowicz, *J. Chem. Phys.* **2017**, *146*, 154105.

[38] G. M. J. Barca, C. Bertoni, L. Carrington, D. Datta, N. De Silva, J. E. Deustua, D. G. Fedorov, J. R. Gour, A. O. Gunina, E. Guidez, T. Harville, S. Irle, J. Ivanic, K. Kowalski, S. S. Leang, H. Li, W. Li, J. J. Lutz, I. Magoulas, J. Mato, V. Mironov, H. Nakata, B. Q. Pham, P. Piecuch, D. Poole, S. R. Pruitt, A. P. Rendell, L. B. Roskop, K. Ruedenberg, T. Sattasathuchana, M. W. Schmidt, J. Shen, L. Slipchenko, M. Sosonkina, V. Sundriyal, A. Tiwari, J. L. Galvez Vallejo, B. Westheimer, M. Włoch, P. Xu, F. Zahariev, M. S. Gordon, *J. Chem. Phys.* **2020**, *152*, 154102.

[39] a) M. Kállay, P. R. Nagy, D. Mester, Z. Rolik, G. Samu, J. Csontos, J. Csóka, P. B. Szabó, L. Gyevi-Nagy, B. Hégely, I. Ladjánszki, L. Szegedy, B. Ladoczki, K. Petrov, M. Farkas, P. D. Mezei, Á. Ganyecz, *J. Chem. Phys.* **2020**, *152*, 074107; b) M. Kállay, P. R. Nagy, D. Mester, Z. Rolik, G. Samu, J. Csontos, J. Csóka, P. B. Szabó, L. Gyevi-Nagy, B. Hégely, I. Ladjánszki, L. Szegedy, B. Ladóczki, K. Petrov, M. Farkas, P. D. Mezei, Á. Ganyecz, MRCC, a quantum chemical program suite, see www.mrcc.hu, **2020**.

[40] K. A. Peterson, T. B. Adler, H. J. Werner, *J. Chem. Phys.* **2008**, *128*, 084102.

[41] D. Figgen, K. A. Peterson, M. Dolg, H. Stoll, *J. Chem. Phys.* **2009**, *130*, 164108.

[42] G. Knizia, T. B. Adler, H. J. Werner, *J. Chem. Phys.* **2009**, *130*, 054104.

[43] a) K. E. Yousaf, K. A. Peterson, *J. Chem. Phys.* **2008**, *129*, 184108; b) S. Kritikou, J. G. Hill, *J. Chem. Theory Comput.* **2015**, *11*, 5269–5276; c) F. Weigend, *J. Comput. Chem.* **2008**, *29*, 167–175; d) J. G. Hill, *J. Chem. Phys.* **2011**, *135*, 044105.

[44] a) A. D. Becke, *Phys. Rev. A* **1988**, *38*, 3098–3100; b) J. P. Perdew, *Phys. Rev. B* **1986**, *33*, 8822–8824.

[45] M. Kállay, P. R. Surján, *J. Chem. Phys.* **2001**, *115*, 2945–2954.

[46] a) Y. J. Bomble, J. F. Stanton, M. Kállay, J. Gauss, *J. Chem. Phys.* **2005**, *123*, 054101; b) M. Kállay, J. Gauss, *J. Chem. Phys.* **2005**, *123*, 214105; c) M. Kállay, J. Gauss, *J. Chem. Phys.* **2008**, *129*, 144101.

[47] S. A. Kucharski, R. J. Bartlett, *J. Chem. Phys.* **1992**, *97*, 4282–4288.

[48] F. Neese, E. F. Valeev, *J. Chem. Theory Comput.* **2011**, *7*, 33–43.

[49] T. H. Dunning, *J. Chem. Phys.* **1989**, *90*, 1007–1023.

[50] J. F. Stanton, *J. Chem. Phys.* **1994**, *101*, 371–374.

[51] K. A. Peterson, D. E. Woon, T. H. Dunning, *J. Chem. Phys.* **1994**, *100*, 7410–7415.

[52] a) C. E. Dykstra, *Chem. Phys. Lett.* **1977**, *45*, 466–469; b) N. C. Handy, J. A. Pople, M. Head-Gordon, K. Raghavachari, G. W. Trucks, *Chem. Phys. Lett.* **1989**, *164*, 185–192.

[53] G. L. Stoychev, A. A. Auer, F. Neese, *J. Chem. Theory Comput.* **2017**, *13*, 554–562.
[54] a) P. Piecuch, M. Włoch, *J. Chem. Phys.* **2005**, *123*, 224105; b) P. Piecuch, M. Włoch, J. R. Gour, A. Kinal, *Chem. Phys. Lett.* **2006**, *418*, 467–474; c) M. Włoch, J. R. Gour, P. Piecuch, *J. Phys. Chem. A* **2007**, *111*, 11359–11382.
[55] S. V. Levchenko, A. I. Krylov, *J. Chem. Phys.* **2004**, *120*, 175–185.
[56] Geometries of the platinum species studied here were taken from reference [5a], the analogous palladium species were obtained with the same methods as used in reference [5b].
[57] a) C. Angeli, R. Cimiraglia, S. Evangelisti, T. Leininger, J. P. Malrieu, *J. Chem. Phys.* **2001**, *114*, 10252–10264; b) C. Angeli, R. Cimiraglia, J.-P. Malrieu, *Chem. Phys. Lett.* **2001**, *350*, 297–305; c) C. Angeli, R. Cimiraglia, J.-P. Malrieu, *J. Chem. Phys.* **2002**, *117*, 9138–9153.
[58] G. H. Booth, A. J. Thom, A. Alavi, *J. Chem. Phys.* **2009**, *131*, 054106.
[59] N. S. Blunt, S. D. Smart, J. A. Kersten, J. S. Spencer, G. H. Booth, A. Alavi, *J. Chem. Phys.* **2015**, *142*, 184107.
[60] G. H. Booth, D. Cleland, A. J. Thom, A. Alavi, *J. Chem. Phys.* **2011**, *135*, 084104.
[61] a) K. Ghanem, A. Y. Lozovoi, A. Alavi, *J. Chem. Phys.* **2019**, *151*, 224108; b) K. Ghanem, K. Guther, A. Alavi, *J. Chem. Phys.* **2020**, *153*, 224115.
[62] K. Guther, R. J. Anderson, N. S. Blunt, N. A. Bogdanov, D. Cleland, N. Dattani, W. Dobrautz, K. Ghanem, P. Jeszenszki, N. Liebermann, G. Li Manni, A. Y. Lozovoi, H. Luo, D. Ma, F. Merz, C. Overy, M. Rampp, P. K. Samanta, L. R. Schwarz, J. J. Shepherd, S. D. Smart, E. Vitale, O. Weser, G. H. Booth, A. Alavi, *J. Chem. Phys.* **2020**, *153*, 034107.
[63] In this work the program version from March 2022 was used.
[64] O. Weser, N. Liebermann, D. Kats, A. Alavi, G. Li Manni, *J. Phys. Chem. A* **2022**, *126*, 2050–2060.
[65] J. J. Eriksen, T. A. Anderson, J. E. Deustua, K. Ghanem, D. Hait, M. R. Hoffmann, S. Lee, D. S. Levine, I. Magoulas, J. Shen, N. M. Tubman, K. B. Whaley, E. Xu, Y. Yao, N. Zhang, A. Alavi, G. K. Chan, M. Head-Gordon, W. Liu, P. Piecuch, S. Sharma, S. L. Ten-No, C. J. Umrigar, J. Gauss, *J. Phys. Chem. Lett.* **2020**, *11*, 8922–8929.
[66] M. Ugandi, M. Roemelt, *manuscript submitted* **2023**.
[67] A. A. Holmes, N. M. Tubman, C. J. Umrigar, *J. Chem. Theory Comput.* **2016**, *12*, 3674–3680.
[68] A. Khedkar, M. Roemelt, *J. Chem. Theory Comput.* **2019**, *15*, 3522–3536.
[69] M. Ugandi, M. Roemelt, *Int. J. Quantum Chem.* **2023**, *123*, e27045.
[70] a) J. L. Rinnenthal, K.-H. Gericke, *J. Mol. Spectrosc.* **1999**, *198*, 115–122; b) Negligible ZPVE contributions below 0.1 kcal mol^{-1} allow comparison with computed total energy differences for the singlet/triplet gap of imidogen.
[71] L. Salem, C. Rowland, *Angew. Chem. Int. Ed.* **1972**, *11*, 92–111.
[72] a) H. Fukutome, *Prog. Theor. Phys.* **1973**, *49*, 22–36; b) H. Fukutome, *Prog. Theor. Phys.* **1972**, *47*, 1156–1180; c) H. Fukutome, *Prog. Theor. Phys.* **1973**, *50*, 1433–1451; d) P.-O. Löwdin, *Phys. Rev.* **1955**, *97*, 1509–1520.
[73] For a related discussion of spin-preserving RHF and ROHF wave functions with broken space symmetry we refer to the work of Paldus: a) X. Li, J. Paldus, *Int. J. Quantum Chem.* **2008**, *108*, 2117–2127; b) X. Li, J. Paldus, *Phys. Chem. Chem. Phys.* **2009**, *11*, 5281–5289; c) X. Li, J. Paldus, *J. Chem. Phys.* **2009**, *130*, 084110.
[74] A detailed comparison of all coupled-cluster codes investigated here is provided as supporting information.
[75] John F. Stanton, University of Florida, Department of Chemistry, Gainesville Florida, personal communication, January 2023.
[76] T. J. Lee, P. R. Taylor, *Int. J. Quantum Chem.* **1989**, *23*, 199–207.
[77] a) A. D. Boese, M. Oren, O. Atasoylu, J. M. L. Martin, M. Kállay, J. Gauss, *J. Chem. Phys.* **2004**, *120*, 4129–4141; b) A. Karton, E. Rabinovich, J. M. L. Martin, B. Ruscic, *J. Chem. Phys.* **2006**, *125*, 144108.
[78] P.-O. Löwdin, *Pure Appl. Chem.* **1989**, *61*, 2185–2194.
[79] We like to reflect here the salient points of detailed discussions with Professor Stanton: It seems that, e. g., in CFOUR the BS-CC solution for singlet imidogen generally converges to a triplet state rather than to the desired broken-symmetry singlet: while the $\langle S^2 \rangle$ expectation value of the UHF reference approaches 1.0 as anticipated, the corresponding projected $\langle S^2 \rangle$ expectation value of the CCSD wave function is about 1.3 and it approaches 2.0 in the CCSDT expansion. Interestingly, spin-projection with the Yamaguchi formula yields results in nearly perfect agreement with FCI data. However, use of the rigorous $\langle S^2 \rangle$ expectation value computed for the CCSD wave function (about 1.6) leads to poor results after spin-projection.
[80] a) J. N. Harvey, *WIREs Comput. Mol. Sci.* **2014**, *4*, 1–14; b) H. Schwarz, *Int. J. Mass Spectrom.* **2004**, *237*, 75–105; c) D. Schröder, S. Shaik, H. Schwarz, *Acc. Chem. Res.* **2000**, *33*, 139–145.

Manuscript received: April 2, 2023
Revised manuscript received: April 27, 2023
Version of record online: May 24, 2023